

https://dspace.org/

The determination of the strength characteristics of wide pillars

Cruise, John Anthony

2015-01-15
http://hdl.handle.net/10539/16554

Downloaded from a DSpace repository. https://dspace.org/

THE DETERMINATION OF THE STRENGTH CHARACTERISTICS OF WIDE PILLARS

BY

JOHN ANTHONY CRUISE

A dissertation presented to the Department of Mining Engineering of the University of the Witwatersrand for the degree of Master of Science in Engineering.

February 1969.

DECLARATION

I, JOHN ANTHONY CRUISE, declare that this dissertation is my own work and has not been previously submitted to another University for degree purposes.

J.A. CRUISE, B.Sc. (Eng.)(Rand)

Date: 17·2·1969

TABLE OF CONTENTS

	Page
Glossary of Terms	
Introduction	
Chapter 1 - Failure of Material	1
1.1 The General Theory of Elasticity.	1
1.2 The Atomic Failure Strength.	2
1.3 The Griffith Crack Theory.	2
1.4 The Modified Griffith Crack Theory.	3
1.5 The Mohr Failure Envelope.	4
1.6 The Theory of Plasticity.	4
Chapter 2 - Failure of Rock Systems Containing Pillars	7
2.1 Homogeneous Isotropic Model.	7
2.2 Poisson's Ratio Effect.	8
2.3 Mohr Effect.	8
Chapter 3 - Stress Distribution	10
3.1 Tributary Area Theory.	10
3.2 Stress Distribution in the Pillar.	10
3.3 Stress Distribution around the Pillar.	11
3.4 Photoelastic Stress Analysis.	12
Chapter 4 - Previous Pillar Formulae	14
Chapter 5 - Derivation of Wide Pillar Formulae	16
5.1 The Strength of Pillar Material.	16
5.2 The Failure Strength of a Unit Pillar.	17
5.3 Strength Multiplication Factor - k_1.	18
5.4 The Lateral Stress Increase Factor - k_2.	19

		Page
5.5	Analysis of a Row of Unit Pillars.	20
5.6	Strip Pillar Analysis.	23
	5.6. 1. Finite Element Approach.	24
	5.6. 2. Continuous Rate of Increase Approach.	25
	5.6. 3. The Comparison of the Finite Element and the Continuous Rate of Increase Approaches.	27
5.7	Square Pillar Analysis.	27
5.8	Circular Pillar Analysis.	30
Chapter 6 - Laboratory Investigation		33
6.1	Description of Material for Laboratory Tests.	33
6.2	Method of Testing Rock Specimens.	33
	6.2. 1. Preparation of Specimens.	33
	6.2. 2. The Testing Procedure to Determine the Specimen Failure Strength.	34
6.3	Influence of Various Factors on the Failure Strength.	35
	6.3. 1. The Isotropy of the Material.	35
	6.3. 2. Griffithc Cracks.	35
	6.3. 3. Vapour Pressure.	35
	6.3. 4. Temperature.	35
	6.3. 5. Rate of Loading.	36
	6.3. 6. The Effect of Interfaces.	36
Chapter 7 - Results		37
7.1	Observation of the Mode of Failure.	37
7.2	Definition of Failure.	38
Chapter 8 - Discussion of Results		39
8.1	Laboratory Tests.	39
8.2	Comparison with Previous Theories.	40
Chapter 9 - Conclusions		44

References

Appendices

I The Determination of k_1 under Elastic Conditions.

II The Determination of k_2 under Elastic Conditions.

III Validity of Approximation of Equal Strengths of all Unit Pillars in the Same Row in the Square Pillar Analysis.

IV Computer Program for Strip Pillar Calculation Using the Continuous Rate of Increase Approach.

V Comparison of the Two Strength Approaches.

VI The Square Pillar Formula as a Continuous Function.

VII Specimen Saturation Times.

VIII The Effect of Interfaces on the Failure Load.

IX Strip Pillar Problem.

X Square Pillar Problem.

XI Circular Pillar Problem.

GLOSSARY OF TERMS

(in order of appearance)

σ_o	strength of material
γ	specific surface energy
E	Young's Modulus
a	space between neighbouring atomic particles
σ_o	maximum stress
σ_a	applied stress
c	½ length of crack
r	radius of curvature at end of crack
ν	Poisson's Ratio
σ_1, σ_2, σ_3	Principal stresses
α	angle of shear plane to the horizontal plane
ϕ	angle of internal friction
σ_p	average pillar stress
σ_o	vertical field stress
R	extraction ratio
p	load distribution
P	total load
a	length of boundary
x	distance from centre
σ	strength of pillar
w	width of pillar
h	height of pillar
k, a, b	constants

R	width to height ratio
σ_u	failure strength of a unit pillar
σ_c	uniaxial compressive strength
k_1	Strength Multiplication Factor
k_2	Lateral Stress Increase Factor
c	$k_1 k_2$
N	number of unit pillars to centre unit pillar of a wide pillar (inclusive)
σ_N	strength of the Nth pillar
n	distance into a wide pillar
σ_n	strength at a point distant n into a wide pillar
σ_{AV}	average strength of pillar
K	constant
σ_o	virgin stress
x	percentage extraction

INTRODUCTION

Throughout the long history of mining *Sub Terra*, the mining engineer's main concern has been support. From the earliest times, the leaving of unmined portions of rock, or pillars, as support, has constituted an integral part of most underground mining operations. It therefore seems paradoxical that, although pillars have been used so extensively, there exists today no adequate generalised calculation to determine the amount of load a pillar can support.

Recently there have been many attempts to establish a pillar strength formula, but in the main these tend either to apply only to a specific material under specific conditions, or to depend on so many parameters and variables that they prove inapplicable in practice.

In the vast majority of pillar applications, the size has been determined by past experience and then trial and error for the specific application. This results in a general "rule-of-thumb", which holds until there are an excessive number of failures.

It is the aim of this dissertation to produce a generalised pillar strength formula for wide pillars, i.e. those whose lateral dimensions are the greatest. It should be noted that it is just the strength of the individual solid pillar that is investigated. It is therefore assumed that the surrounding strata is competant, such that it will not fail prior to pillar failure nor does it induce undue high stress concentrations in the pillar due to external phenomena, nor does the pillar partially fail before ultimate failure.

CHAPTER 1

FAILURE OF MATERIAL

1.1. THE GENERAL THEORY OF ELASTICITY

In the field of rock mechanics most calculations are based on the assumption that rock behaves elastically. Invariably the question arises as to whether this assumption is valid.

Apart from the fact that there exists no other theory which is as complete and computable, it has been found by many authors that the stress/strain curve for rock is linear. Moreover, a according to Coates[1], where the rock is visco-elastic and elasto-plastic, it can be considered to behave according to a modification of the elastic theory, having the same stress-equilibrium equations and boundary conditions and differing only in the compatability equations.

Hence, as the most applicable and the most complete theory available, elasticity is a good first approximation to describe rock behaviour.

An insight into the theory of elasticity can be found in most textbooks dealing with fundamental strength of materials. Two, regarded as the classical textbooks in this field, are written by Timoshenko and Goodier[2] and Muskhelishvili[3].

In this dissertation the theory of elasticity is used extensively to express and relate stress and strain conditions.

1.2. THE ATOMIC FAILURE STRENGTH

In considering the failure strength of materials microscopically, the lower limit of consideration is the strength due to the cohesion of atomic particles. Orowan[4] gives the strength of material as :-

$$\sigma_o = \sqrt{\frac{2\gamma E}{a}}$$

where γ = specific surface energy

E = Young's modulus

a = space between neighbouring atomic particles

However, the strength of a substantial mass of material is found to be much lower than the atomic strength. This gave rise to the Griffith Crack Theory.

1.3. The Griffith Crack Theory

Griffith[5] assumed that the difference between the atomic tensile strength and the massive tensile strength was due to high stress concentrations around small cracks inherent in massive material.

These high stress concentrations cause the cracks to propagate, finally resulting in the failure of the material along the cracks and their propagations.

Approximating a crack two-dimensionally by an ellipse of large eccentricity, Griffith calculated the maximum stress at the end of the crack, orientated at right angles to the applied tension, from the equation:

$$\sigma_o = 2\sigma_a \frac{c}{r}$$

where σ_a = applied tensile stress

$2c$ = length of crack

r = radius of curvature at the end of the crack

To relate the propagation of cracks to the constants of the material Griffith considered the energy balance during crack propagation. The types of energy which have to be considered are:

(a). A loss in potential energy due to displacements - P.E.

(b). A gain in strain energy around the crack - E.E.

(c). A gain in surface energy due to formation of new crack areas - S.E.

(d). A gain in kinetic energy due to crack propagation - K.E.

(e). A gain in potential energy due to plastic deformation - Pl.E.

The energy balance is therefore expressed by the equation,

$$P.E. = E.E. + S.E. + K.E. + Pl.E.$$

For the stable crack propagation the surface energy gained in rupturing the molecular bonds along the crack path must be equal to the nett reduction in the strain energy of the system,

$$\text{i.e.} \qquad S.E. = E.E.$$

In three-dimensions a flat oblate ellipsoid was studied by Sack[6] who derived the expression

$$\sigma_a = \frac{E}{2c(1-\nu^2)}$$

where E = Young's Modulus

ν = Poisson's Ratio

2c = crack length

In compression the original Griffiths theory does not make allowances for the closure of very flat cracks before they reach a high enough stress to propagate. The frictional forces which come into being when the faces of the crack come into contact exert a marked influence on the crack behaviour.

1.4. THE MODIFIED GRIFFITH CRACK THEORY

To study the effect of friction on closed crack surfaces McClintock and Walsh[7] adapted the Griffith theory by making

the assumption that the initial crack in an unstressed body is uniformly closed over its whole length, i.e. the stress required to close the crack is zero

For negative stress i.e. tensile stress the original Griffith Theory holds, and for positive stress i.e. compressive stress the Modified Griffith Theory holds. The transition point of the two theories occurs at zero stress as indicated in Fig. 1.

1.5. THE MOHR FAILURE ENVELOPE

A 2-dimensional stress system in an elastic body (see Fig. 2a) can be illustrated graphically by a Mohr circle (see Fig 2b).

As the stress difference increases the radius of the circle increases. For a fixed minimum stress a maximum radius is reached at failure. If the semi-circles at failure for different minimum stress values are plotted they are found to have a common envelope called the Mohr failure envelope which is also shown in Fig. 2 (b). States of active and passive failure can also be derived from the Mohr diagram as discussed in more detail in section 2.3. The Griffith and Mohr theories were derived for elastic materials. For plastic materials useful theories have been proposed by Tresca and von Mises.

1.6. THE THEORY OF PLASTICITY

Under certain stress conditions rock is known to behave plastically. The complexity of plastic behaviour, the change of phase from elasticity to plasticity and the wide variation in various materials contribute to the reason why the theory of

/plasticity

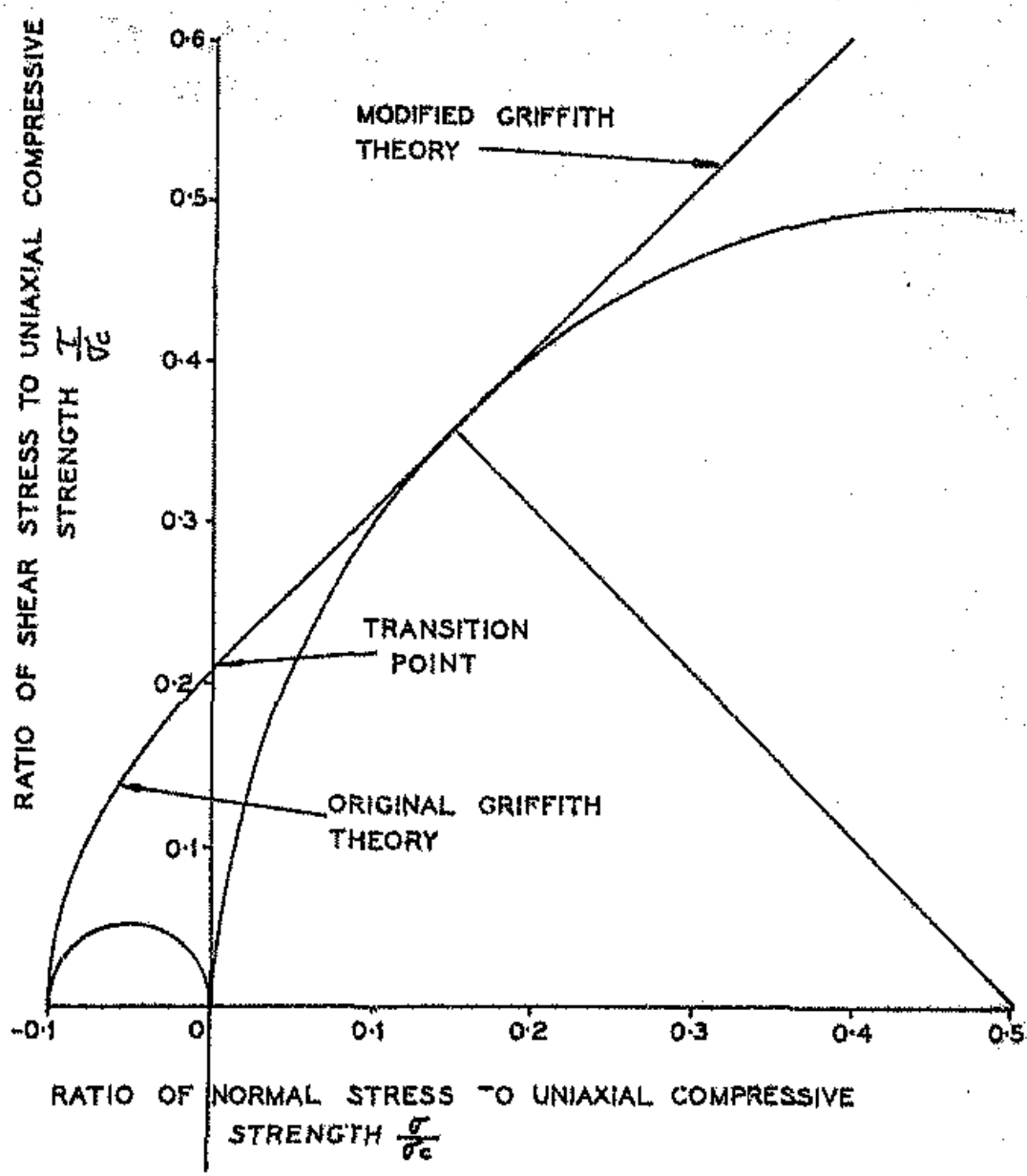


FIGURE 1. MOHR ENVELOPE FOR ORIGINAL AND MODIFIED GRIFFITH'S BRITTLE FRACTURE CRITERIA IN TERMS OF THE UNIAXIAL COMPRESSIVE STRENGTH σ_c FOR $\mu = 1{\cdot}0$. (AFTER HOEK [20])

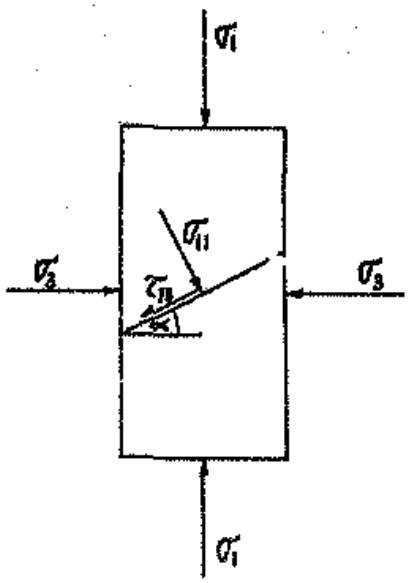


FIGURE 2a. TWO-DIMENSIONAL STRESS SYSTEM ON AN ELASTIC BODY.

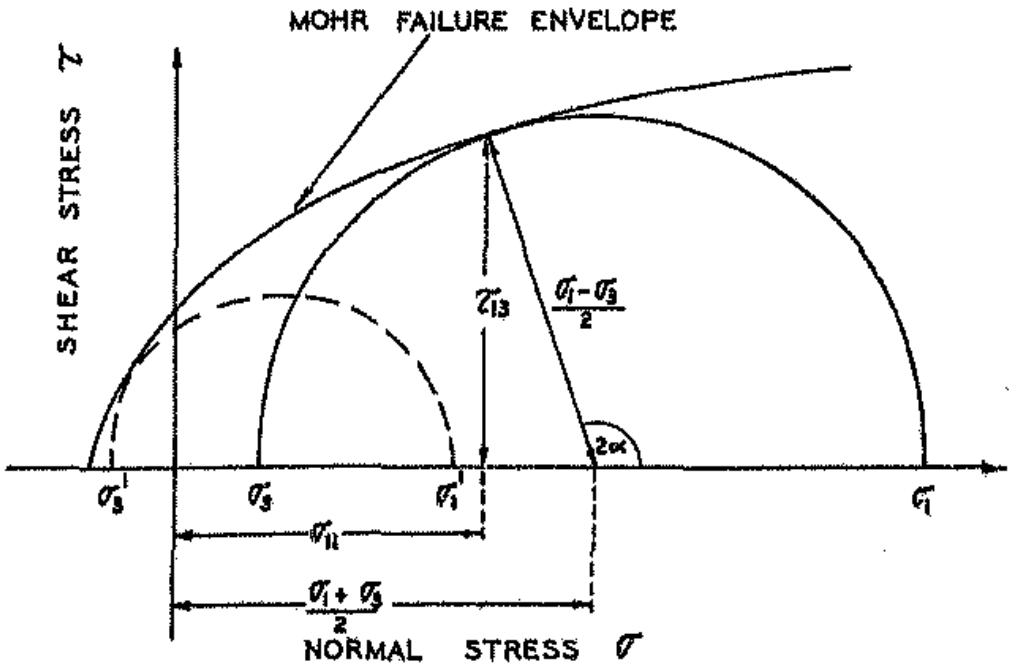


FIGURE 2b. MOHR DIAGRAM SHOWING THE RELATIONSHIP BETWEEN THE STRESSES ON A TWO-DIMENSIONAL ELASTIC BODY AT FAILURE, AND THE COMMON FAILURE ENVELOPE FOR FAILURE AT VARIOUS STRESSES.

plasticity has not developed into a rigorous discipline. In spite of this some attempts have been made to bring plasticity on a par with elasticity. According to Hoffman and Sachs[8], two theories have been propounded to explain the failure of material in plasticity viz. that of Tresca - St. Venant and that of von Mises - Hencky. Both theories use yield surfaces to describe failure. They differ in that Tresca - St. Venant proposes that the yield surface is hexagonal and von Mises - Hencky that it is elliptical (see Fig. 3).

The discrepancy is two conditions:-

(a). the maximum-shearing-stress conditions of Tresca - St. Venant assumes six different expressions in various regions of the $\sigma_1\sigma_2$ plane, depending on the relative magnitudes and signs of σ_1 and σ_2. This gives an hexagon failure surface as shown in Fig. 3.

(b). the strain-energy-of-distortion condition of von Mises - Hencky is an ellipse with the major and minor axes bisecting the σ_1- and σ_2- axes and passing through the vertices of the hexagon of the maximum-shearing-stress condition.

The two conditions predict the same yield strength for equal biaxial stresses given by $\sigma_1 = \sigma_2 = \pm \sigma_0$, represented by B and E and for uniaxial stress, A, C, D, F in Fig. 3.

The maximum deviation of the two theories occurs for pure shear, $\sigma_1 = -\sigma_2$.

The values are then,

Maximum-shearing-stress	$\sigma_1 = -\sigma_2 = \pm \frac{\sigma_0}{2}$
Strain-energy-of-distortion	$\sigma_1 = -\sigma_2 = \pm \frac{\sigma_0}{\sqrt{3}}$

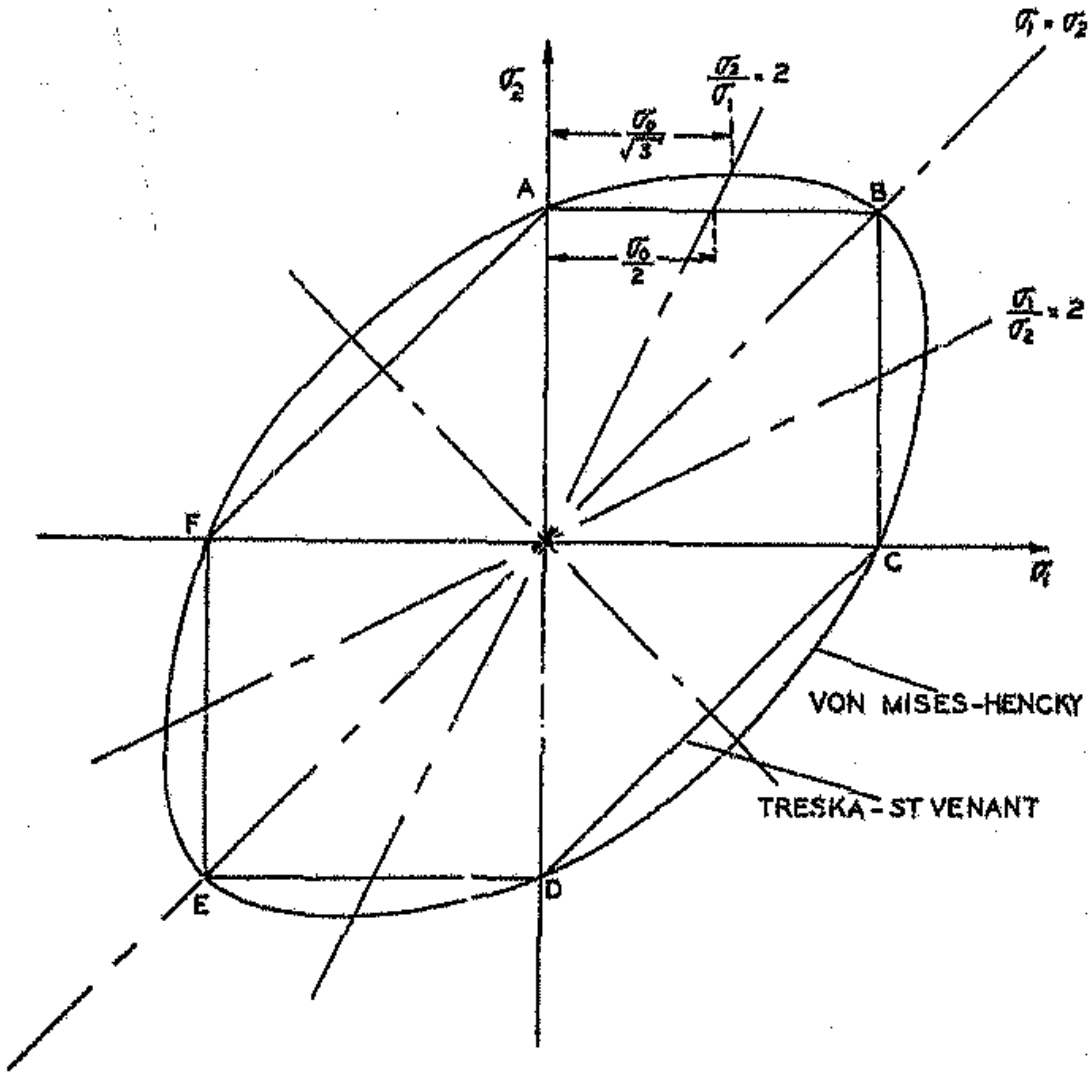


FIGURE 3. COMPARISON OF THE TWO YEILD SURFACE FAILURE THEORIES IN PLASTICITY (AFTER HOFFMAN AND SACKS[8])

Briefly the failure criteria can be summarised as:

(a). the general theory of elasticity is still the most extensive and the most easily applicable theory to date.

(b). the atomic strength, though valid for microscopic order of analyses fails for the macroscopic state.

(c). the modified Griffith Theory can in general be applied to calculate the strength of rock, however, its application is limited as reliable values for surface free energy are not available.

(d). the Treska-von Mises theories will be useful in later determinations of strength when more is known about the plasticity of rock, but for the purpose of this dissertation the assumption is made that rock behaves elastically.

CHAPTER 2

FAILURE OF ROCK SYSTEMS CONTAINING PILLARS

In order to apply mathematical theory of elasticity to practical mining conditions Salamon[9] considers four types of idealised models viz:-

(a). Homogeneous isotropic model.

(b). Homogeneous transversely isotropic model.

(c). Frictionless laminated model.

(d). Multimembrane model.

To eliminate tedious mathematical calculations it will be assumed in this dissertation that the mining condition can be simulated by the homogeneous isotropic model.

2.1. HOMOGENEOUS ISOTROPIC MODEL

To apply this model it is assumed that the mechanical properties of all portions of the rock mass is the same, and their magnitude is independent of the direction of loading i.e. the model disregards the possible effect of the bedded nature of the rock. It provides a useful approximation in the case of deep-seated hard rock, where the bedding is not pronounced and no preferential direction with regard to its properties exists.

The basis of calculation is on the mirror image concept with only two parameters to define the mechanical properties of the material viz. Young's Modulus E and Poisson's Ratio ν. The mirror image concept satisfies the condition of shear stress-free ground surface by superimposing the solution for an element at

/infinite

infinite depth on its mirror image. The surface is freed of normal stress by the addition of another stress function.

2.2. POISSON'S RATIO EFFECT

The stress on a pillar increases with progressive mining due to the weight of the overlying strata, and the increase causes a deformation of the pillar. As the pillar deforms vertically, it expands laterally until it fails by splitting vertically and sliping of the outer layers. This continues until the size of the pillar is so small that it can no longer bear the weight of the overlying strata and it fails violently.

The lateral expansion occurs as a result of the Poisson's Ratio Effect which is unrestricted at mid-height of the pillar and restricted on the hangingwall and the footwall contacts with the pillar. This causes bulging at the mid-height and leads to vertical cracking (see Fig.4).

2.3. MOHR EFFECT

If the pillar is slender enough, an oblique shear plane tends to develop. (see Fig. 5a). This is explained by Terzaghi and Peck[10] in the theory of active and passive shear planes and it can be analysed by the Mohr Rupture Theory.

Briefly, the angle α of the shear plane (see Fig. 5a) to the horizontal plane is $45^{\circ} + \frac{\phi}{2}$ where ϕ is the angle of internal friction. ϕ depends on the difference between the applied vertical stress σ_v and the restricting horizontal stress σ_h (see Fig. 5b).

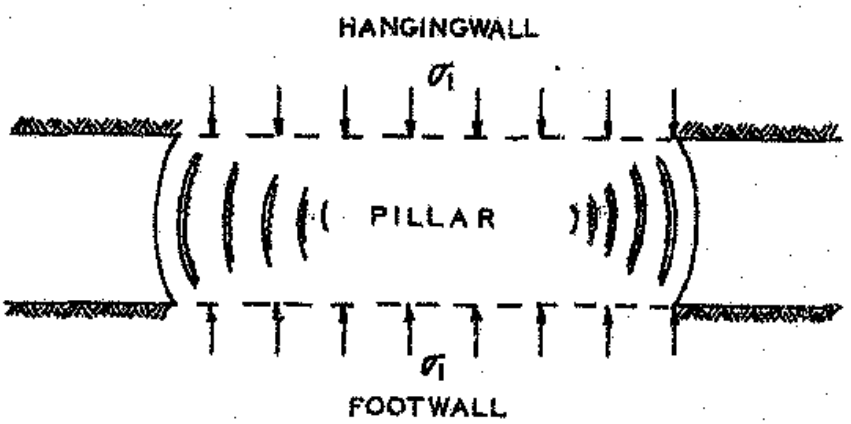


FIGURE 4. CROSS SECTION OF A PILLAR SHOWING THE POISSON'S RATIO EFFECT PRODUCING BULGING AT MID-HEIGHT AND VERTICAL CRACKING WHEN SUBJECTED TO VERTICAL STRESS - σ_1.

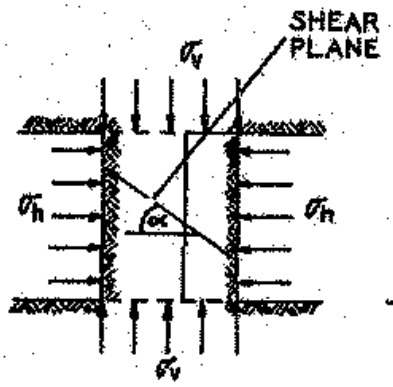


FIGURE 5a.

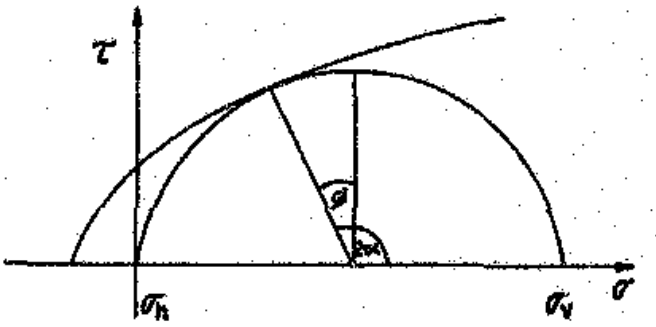


FIGURE 5b.

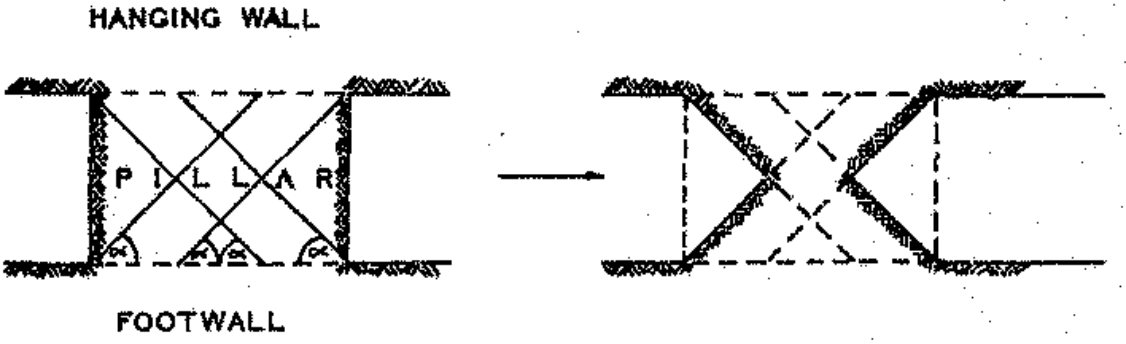


FIGURE 5c.

FIGURE 5d.

THE MOHR EFFECT SHOWING THE DEVELOPMENT OF SHEAR PLANES AND THEIR EFFECT ON A WIDE PILLAR.



FIGURE 5e.

COMBINATION OF POISSON'S RATIO EFFECT AND MOHR EFFECT.

According to the Mohr theory a number of shear planes are induced, all having the same angle to the horizontal. Some will have the opposite sign (see Fig. 5c).

This causes the "waist" effect commonly seen in coal pillars, due to the loose rock falling away (see Fig. 5d).

In practice what is observed is, firstly a bulging effect and then the rock at mid-height falls away, leaving, not a clean shear plain, but a jagged surface. This could be explained by a combination of Poisson's Ratio Effect and the Mohr Effect (see Fig. 5e).

However, it could be due to the nature of the material.

CHAPTER 3

STRESS DISTRIBUTION

In determining the strength of material the most commonly used method is to study its reaction to an applied stress. Hence, the knowledge of the exact nature of the applied stress is imperative. Two factors of this nature are important viz. the amount of stress and its distribution.

3.1. TRIBUTARY AREA THEORY

To measure the total amount of stress under mining conditions the tributary area theory provides a fairly accurate and easily manipulative estimate. This theory states that the pillar supports the entire weight of rock above the pillar and above the excavation tributary (or adjacent) to it. This can be expressed by the equation

$$\sigma_p = \frac{So}{1 - R}$$

where σ_p = average pillar stress

So = vertical field stress

R = extraction ratio

Hence this method gives the maximum average stress that can occur in the pillar.

3.2. STRESS DISTRIBUTION IN THE PILLAR

If there is a non-uniform stress distribution in the pillar, then the maximum stress is not that given by the tributary area theory, but a greater value. As the rock will fail first at the stress of greatest value, it is important to know the configuration of the stress distribution.

Timoshenko[2] gives the load distribution on a straight boundary (see Fig. 6a) as $P = \frac{P}{\pi\sqrt{a^2 - x^2}}$

where P = total load

a = length of boundary

x = distance from centre

A similar configuration is given by Salamon and Oravecz[11] for the stress distribution over a pillar (see Fig. 6b). They maintain that this applies both to the homogeneous isotropic model and the transversely isotropic model, the only difference being the choice of the appropriate physical constants in the final results.

An approximation that is used in this approach is, that at any point over the pillar, the vertical stress is proportional to the pillar convergence there. From this it is calculated that the stress convergence at the corners of the pillar is 37.5% higher than the mean stress over the whole pillar.

Coates[1] gives the more likely stress distribution as having the maximum stress at a distance into the pillar (see Fig. 6c). In practice the partial fracturing from blasting or release of confinement of the surface rock, produces a zone commonly 2 feet to 6 feet thick that can sustain little stress. The peak stress concentration is thus moved to the edge of the unfractured portion of the pillar.

3.3. STRESS DISTRIBUTION AROUND THE PILLAR

Coates[1] maintains that the stress distribution with the footwall and the hangingwall of the same moduli of deformation

/is

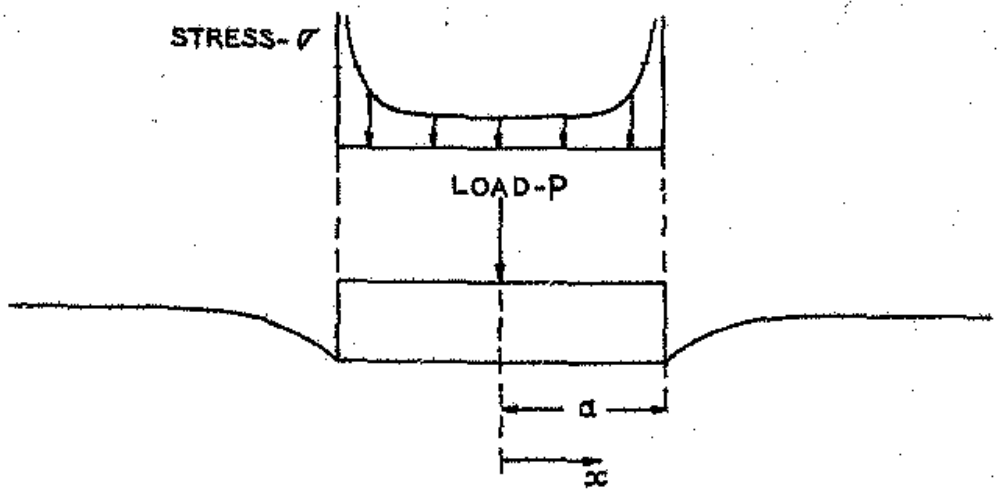


FIGURE 6a. STRESS DISTRIBUTION OVER A STRAIGHT BOUNDARY PRODUCING CONSTANT DEFLECTION (AFTER TIMOSHENKO[2]).

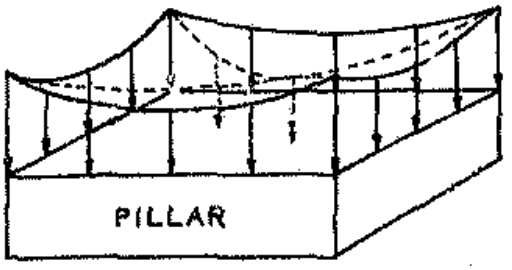


FIGURE 6b. STRESS DISTRIBUTION OVER A PILLAR (AFTER SALAMON AND ORAVECZ[1]).

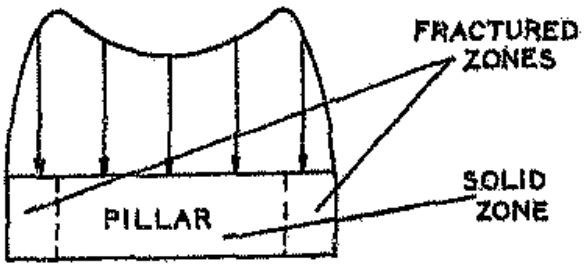


FIGURE 6c. STRESS DISTRIBUTION OVER A PILLAR CROSS SECTION (AFTER COATES[1]).

is the same in the footwall on contact with the pillar as the pillar. This is to be expected if one accepts the continuity of stress. So considering the ideal elastic situation the stress will be that of the pillar (see Fig. 7a).

At a distance into the footwall the stress distribution is spread over a larger area and thus the stress concentration is diminished (see Fig 7b), until at a certain distance above or below the pillar it approaches the primitive stress configuration.

N.B. All references to the footwall apply equally to the hangingwall.

Terzaghi and Peck[10] give the floor reaction to pressure on a plate as the development of shear planes (see Fig.7c). This phenomenon is well known in Soil Mechanics.

It was from this concept that Wiggill[12] deduced the stress lines around an open excavation (see Fig. 7d).

3.4. PHOTOELASTIC STRESS ANALYSIS

From photoelastic stress studies on pillar configurations Logie[13] arrived at the following conclusions:-

(a). the maximum stress in the pillar occurs at the intersection of the three orthogonal planes viz. the corner of the two sidewalls and the footwall (shown previously by Salamon and Oravecz[11]). This maximum is not affected by the slenderness of the pillar, but by the variation in percentage extraction.

(b). the rate of change of the maximum stress with the precentage extraction is large, obeying approximately linear law.

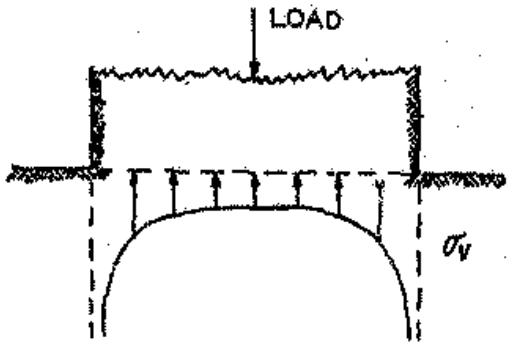


FIGURE 7a.

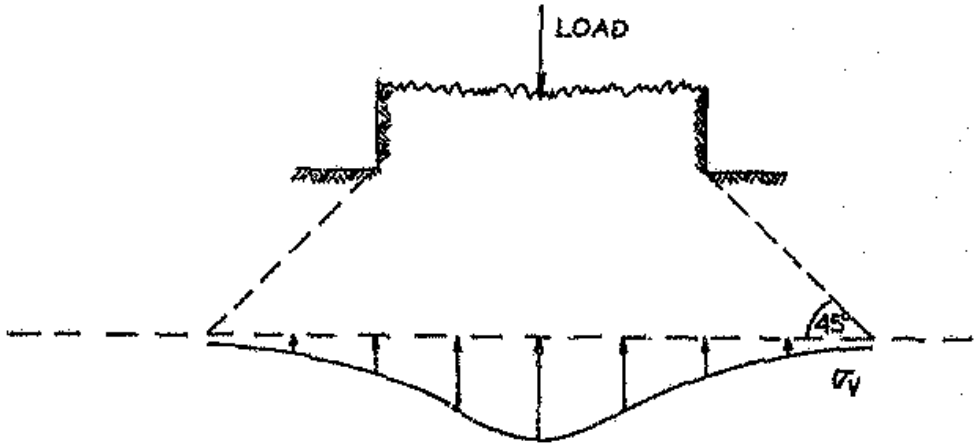


FIGURE 7b.

FIGURES 7a AND 7b. STRESSES IN WALLS ADJACENT TO PILLARS (AFTER COATES [1])

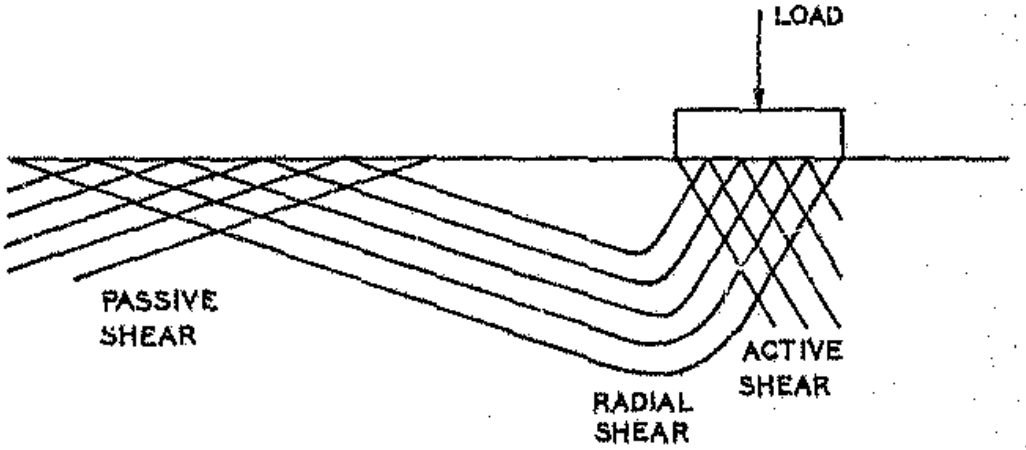


FIGURE 7c. FLOOR REACTION TO PRESSURE ON A PLATE (AFTER TERZAGHI AND PECK[10])

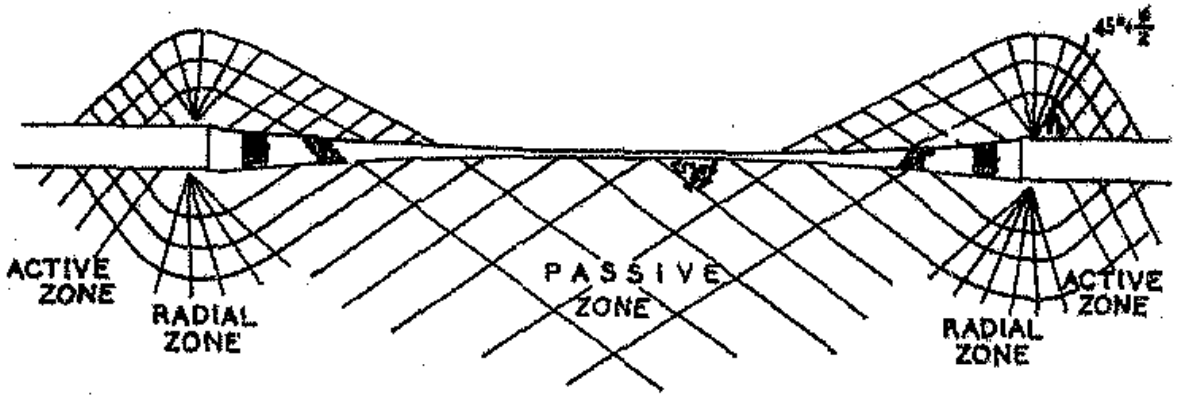


FIGURE 7d. DIAGRAMMATIC SKETCH SHOWING SHEAR ZONES AROUND A STOPING EXCAVATION (AFTER WIGGILL[12])

(c). a tensile stress is produced in the footwall of the excavation of the order of the primitive stress.

(d). for percentage extraction less than 55% the rate of change of the maximum stress at mid-height is relatively small. For greater than 55% extraction the rate is high.

He also shows that across the pillar the stress distribution remains uniform at a distance into the pillar greater than half the height (see Fig. 8).

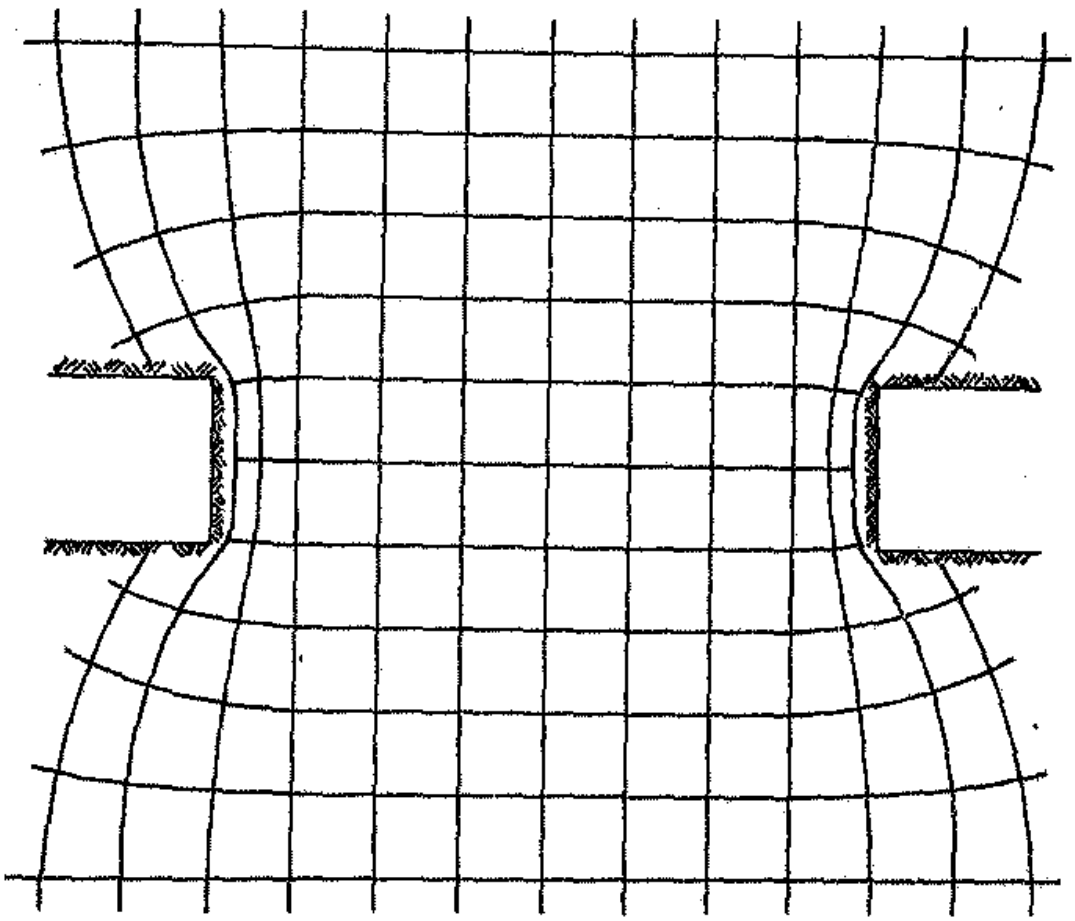


FIGURE 8. DISTRIBUTION OF THE PRINCIPAL STRESS TRAJECTORIES AROUND A WIDE PILLAR (AFTER LOGIE[13])

CHAPTER 4

PREVIOUS PILLAR FORMULAE

As that section of the mining industry which has for some time predominately used the pillar as an integral part of its mining method, the coal mines were the first to become interested in the determination experimentally of the strength of pillars. As far back as 1938 experiments were conducted in the Pittsburgh Coal Beds by Greenwald, Howarth and Hartmann[14] to investigate parameters that might affect the strength. They observed that size had a distinct effect on the strength. From the results of seven tests carried out on in situ square coal pillars, they postulated the form of the equation that relates the size to the strength as being a power function i.e. the strength of a pillar is a function of its width and its height to certain powers.

viz. $$\sigma = k\, w^{a}\, h^{b}$$

where σ = strength of pillar

w = width of pillar

h = height of pillar

k, a, b = constants

Until very recently, this was the accepted form of the pillar strength formulae. Later researchers merely differed with respect to the constants.

However, due to the empirical nature of evaluating, the constants vary considerably, due to the particular nature of the coal specifically tested by individual researchers. The researchers also differed in their approach to the determination of the constants.

Steart[15], in 1954, conducted experiments on laboratory sized specimens and extrapolated the results from the formula he obtained to describe the strength of mine pillars. In 1967, Salamon and Munro[16] approached the problem of pillar strength by a method different from that of simulating a pillar failing in the laboratory. They took a large number of pillars in a number of mines and, on the basis of classing those which had already failed as being too small and those which still stood and carried load as being on the large size, they found the optimum values for the constants statistically using the power function formula as the basic form. Also in 1967 Bieniawski[17] conducted a series of tests on in situ small coal pillars by artificaally inducing a load on the pillars by means of hydraulic jacks, thus simulating pillar failure under safe conditions. Again he used the power function formula as the basic template and gave a new evaluation of the constants.

Thus the various postulates can be summarised by the following table of the constants.

	a	b
Greenwald et al	0.50	-0.83
Steart	0.50	-1.00
Salamon and Munro	0.46	-0.66
Bieniawski	0.16	-0.46

The constant k depends on the nature of the coal . l as it can be seen from the form of the power function formula, it is the value of the strength of a unit cube of coal.

In a later paper in 1967, Bieniawski[18] first deviated from the power function formula by proposing a linear relationship of the form $\sigma = a + bR$

where σ = strength of pillar, R = width to height ratio

$a = 400$, $b = 220$

An evaluation of the merits and limitations of these formulae is given in section 8.1.

CHAPTER 5

DERIVATION OF WIDE PILLAR FORMULAE

5.1. THE STRENGTH OF PILLAR MATERIAL

The strength of pillar material, usually rock, depends on intrinsic parameters and variable external factors, many of which have not yet been identified, let alone analysed.

In attempting an analysis of factors determining the strength of pillar material one must first consider its general nature. The rock may have a structure ranging from separate particles bonded weakly together to a fused glass-like structure, depending on its geological origin and history - whether igneous, sedimentary, or metamorphic; of what elements it is composed; in what array the elements are bonded together and at what stage of metamorphosis. Sandstone is an example of crystals of rock bonded together by a cement weaker than the individual crystals, whereas pure quartzite has been fused so that the importance of individual grains is greatly diminished.

The behaviour of rock under stress may range from purely elastic to plastic or viscous and is of importance in the comparison of different rock types; and even in a single specimen the deformation phase may change noticeably under varying conditions.

The mode of failure of rock may range from a gradual flow to a violent rupture with or without cracking and crumbling. After failure the rock fragments may be recompacted to attain a capacity to once more withstand stress.

The strength of a rock mass is effected by the degree of saturation, chemical alteration, microscopic or macroscopic flaws, internal stress concentrations and rheological deformation. For example, Wiid[19] found that the strength of sandstone decreases markedly with an increase in the percentage saturation; visual chemical alteration occurs at serpentine dykes exposed in underground workings; planes of weakness such as faults, fissures and slips are common occurances in underground workings; the high stress concentration at peninsula abutments left by longwall mining on the Witwatersrand gold mines may cause violent failures; and the rheological deformation under a constant load too low to induce immediate failure has been observed to lead to failure in salt and potash mines.

5.2. THE FAILURE STRENGTH OF A UNIT PILLAR

In mining it has been observed that the strength of a pillar is influenced by its dimensions, more especially so, its least dimension. If the least dimension is its width, it is a "slender pillar" and its strength analysis would be akin to that of "column theory" used in structural engineering.

If the least dimension is its height it is a "wide pillar". In analysing a wide pillar the concept of a unit pillar is used to serve as the foundation upon which the failure strength theory is built. A unit pillar is a cubic pillar of sidelength equal to the height of a wide pillar. Hence *all wide pillars contain* at least one unit pillar. By increasing the unit pillar in its lateral dimensions it becomes a wide pillar.

The failure strength of a unit pillar, σ_u, is taken to be the maximum load per unit area which the pillar can support before failing.

This failure strength should not be confused with the uniaxial compressive strength, σ_c, which is determined by an internationally standardised procedure on a rock specimen of specific size viz. a cylinder of rock of diameter 1.5" and length 3.25". However, the unit strength can be considered to be a function of the uniaxial compressive strength.

$$\text{i.e.} \quad \sigma_u = f(\sigma_c)$$

To date this relationship has not been determined, though a first approximation can be made empirically by conducting a series of tests on specimens of varying size and then extrapolating. It is generally accepted that as the size increases so the strength decreases. However, it is thought that above a certain size, a matter of inches when dealing with metals and feet with coal (Bieniawski[18]), the strength of a cube becomes constant. Recent results (Grobbelaar [21]) indicate that it is possible to estimate the strength of a unit pillar by using the strength of small specimens and observations of crack frequencies.

5.3. STRENGTH MULTIPLICATION FACTOR - k_1.

In nature where one deals with finite bodies, one rarely comes into contact with pure uniaxial stress conditions. Due to the intrinsic nature of materials, being constructed of molecules that are connected to one another by some or other means, one finds, even in the smallest elements, a three-dimensional stress situation. In this three-dimensional stress condition any one of three principal stresses is influenced by the other two. Any change in the magnitude of any one principal stress produces a change in the magnitudes of the other two.

If the unit pillar is considered to be an integral unit with the principal stresses σ_1, σ_2, σ_3 acting on its surfaces (see fig 9a), the change in σ_1, $\Delta\sigma_1$, is a function of the stresses in σ_2 and σ_3, $\Delta\sigma_2$ and $\Delta\sigma_3$ if there is no deformation in the direction of σ_1.

$$\text{i.e.} \quad \Delta\sigma_1 = f(\Delta\sigma_2, \Delta\sigma_3)$$

If the situation is simplified to that of two principal stresses, the maximum and the minimum, σ_1 and say σ_3 in the case of a unit pillar under vertical load we get the relationship

$$\Delta\sigma_1 = f(\Delta\sigma_3)$$

Over small increments this relationship can be approximated by a straight line which has the slope k_1 corresponding to the slope of the curve at that point

$$\Delta\sigma_1 = k_1\Delta\sigma_3 \quad \text{(see Appendix 1).}$$

The effect of this on the unit pillar is that an increase in the lateral stress, increases the failure strength. By definition, the failure of a unit pillar, σ_u, occurs in the uniaxial stress condition i.e. the lateral stress is zero. Therefore, if we apply a stress $\Delta\sigma_3$ we get an increase in σ_u of $k_1\Delta\sigma_3$.

$$\begin{aligned} \text{i.e.} \quad \text{when } \sigma_3 = 0 \qquad & \sigma_1 = \sigma_u \\ \text{when } \sigma_3 = \Delta\sigma_3 \qquad & \sigma_1 = \sigma_u + \Delta\sigma_1 \\ & = \sigma_u + k_1\Delta\sigma_3 \end{aligned}$$

(See fig. 9b and 9c).

5.4. THE LATERAL STRESS INCREASE FACTOR - k_2

Materials, when subjected to a vertical load, show a tendency to deform; in general, by contracting vertically and expanding laterally. The amount of deformation and the ratio between the volumetric deformation vertically to that of horizontally depends on the nature of the material.

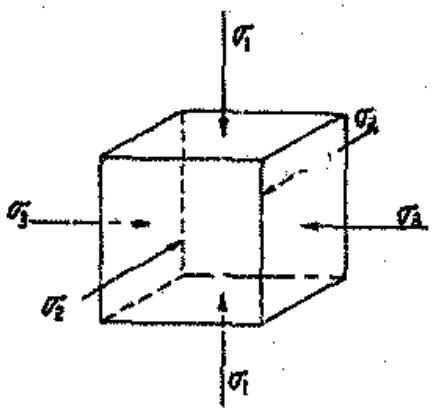


FIGURE 9a. THE PRINCIPAL STRESSES ACTING ON A UNIT CUBE

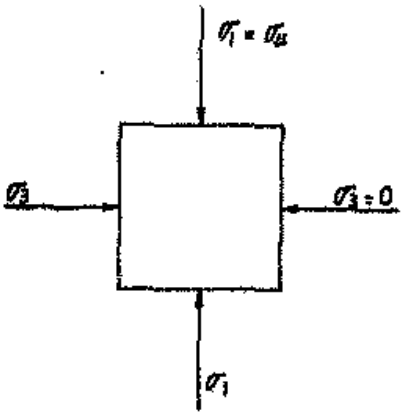


FIGURE 9b. THE TWO-DIMENSIONAL STRESSES FOR A SOLITARY UNIT PILLAR AT FAILURE.

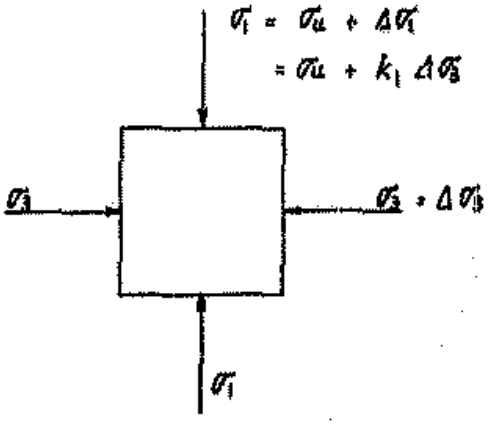


FIGURE 9c. THE EFFECT ON THE VERTICAL FAILURE STRESS (σ_1) BY APPLYING A HORIZONTAL STRESS ($\sigma_3 + \Delta\sigma_3$) ON A TWO-DIMENSIONAL UNIT PILLAR.

For any elastic material these characteristics are generally constants. The values of these properties for a given material can change as the material changes state, from viscous through plastic to elastic for instance, but in general, they can be treated as different constants for each state of material.

If the material is restrained laterally when subjected to a vertical stress, a lateral stress is induced, which is a function of the vertical stress

$$\sigma_3 = f(\sigma_1)$$

Again, the relationship becomes that of a straight line for increments of stress change, giving

$$\Delta\sigma_3 = k_2 \Delta\sigma_1$$

where k_2 is the lateral stress increase factor.

k_2 varies according to the specific material, the stress condition and the state of the material. In general, $0 \leq k_2 \leq 1$

For elastic material $0 < k_2 \leq \frac{\nu}{1-\nu}$

For elastic material under plane strain $k_2 = \frac{\nu}{1-\nu}$

For elastic material under plane stress $k_2 = \nu$

where ν is Poisson's Ratio

(See Appendix 11)

In short the effect of k_2 on the unit pillar is that, if it is restrained, it exerts a lateral stress which is proportional to the vertical stress (see Fig.10).

5.5. ANALYSIS OF ROW OF UNIT PILLARS

As previously stated a wide pillar consists of at least one unit pillar. Taking the unit pillar as an integral entity, consider the effect of a unit pillar on its neighbouring unit pillar within a wide pillar. Being adjacent to one another they provide, a

/mutual

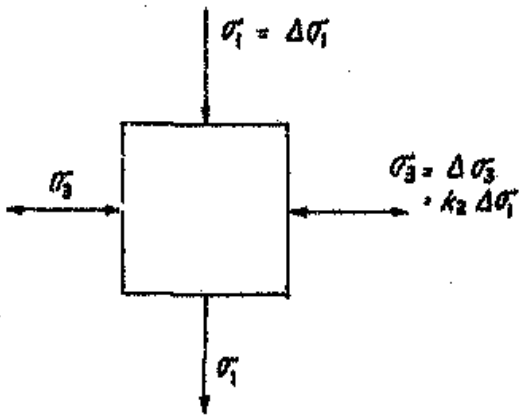


FIGURE 10 THE EFFECT ON THE HORIZONTAL STRESS (σ_3) BY APPLYING A VERTICAL STRESS ($\sigma_1 = \Delta\sigma_1$) ON A HORIZONTALLY RESTRAINED TWO-DIMENSIONAL UNIT PILLAR.

mutual restraint if they do not move laterally. This mutual restraint produces a lateral stress when the pillar complex is subjected to a vertical load, thus increasing the unit pillar's capacity to carry the load; in effect, increasing its strength. Moving in from the perimeter of the wide pillar to its centre, the strength increase becomes cumulative and reaches a maximum in the centre of the pillar.

To illustrate this effect consider three unit pillars. If these pillars are not in contact, we should expect each to have a strength per unit area of σ_u. Hence, we expect all three to fail simultaneously when the load per unit area becomes σ_u. (See Fig.11a).

If the three unit pillars are placed in contact in a row (see Fig. 11b), the two outer pillars would have a restraining effect on the centre one in the σ_3- direction but not in the σ_2- direction. Hence we expect a slight increase in the strength of the centre pillar since it has one less dimension to fail into. However, the strength increase is slight (Practically found to be about 10% in the case of sandstone, see Appendix 111) as it can still fail in the σ_2- direction.

If the three unit pillars form a cross-section of a strip pillar (see Fig.11c), the centre pillar is restrained in the σ_3- direction by the two outer pillars and in the σ_2- direction by similar sets of pillars adjacent to it. This restraint on all sides makes a marked increase in its strength (150% in the case of sandstone see Appendix 111). This increase in strength is due to the development of lateral stress which is k_2 times the unit pillar strength and produces a strength multiplication factor of k_1 times the lateral stress.

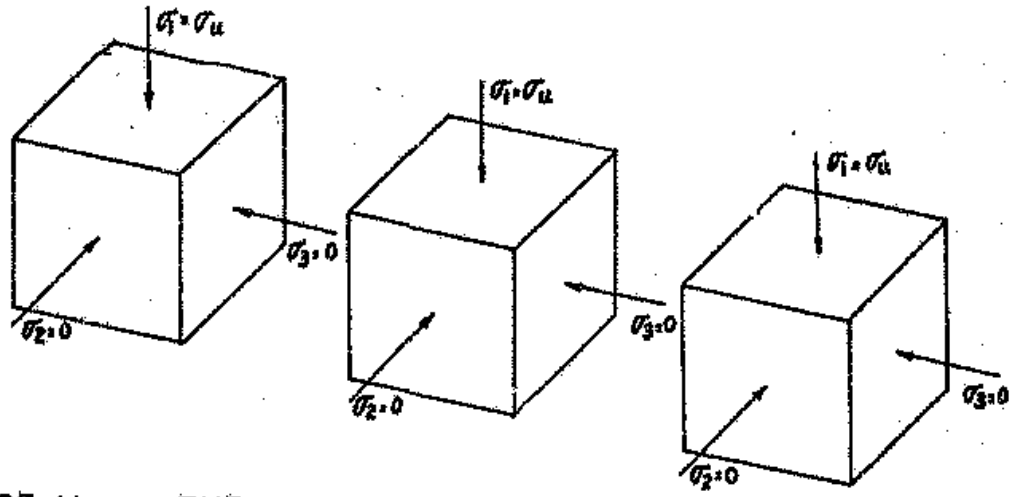


FIGURE 11a. THE STRESSES ON THREE INDEPENDENT UNIT PILLARS AT FAILURE.

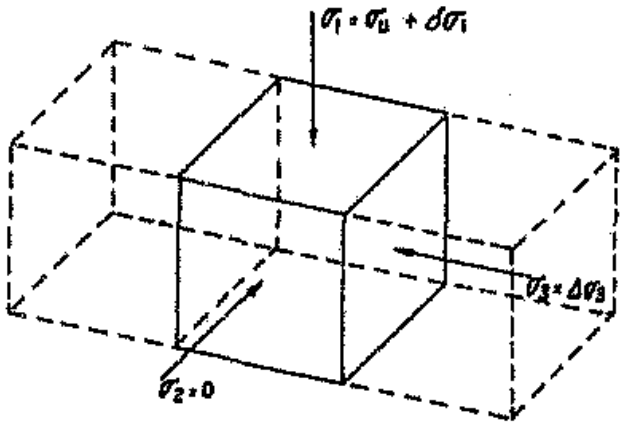


FIGURE 11b. THE EFFECT ON THE STRESSES ON THE CENTRE UNIT PILLAR WHEN RESTRAINED IN THE σ_3 - DIRECTION BY ADJACENT UNIT PILLARS.

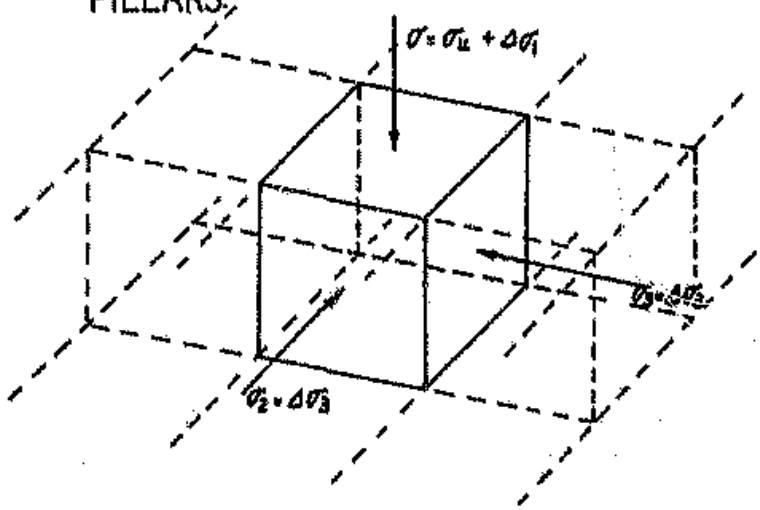


FIGURE 11c. THE EFFECT ON THE STRESSES ON THE UNIT PILLAR WHEN RESTRAINED EQUALLY IN THE σ_2 – AND σ_3 - DIRECTIONS BY ADJACENT UNIT PILLARS.

Hence, the strength for the centre unit pillar increases by $k_1 k_2 \sigma_u$ giving the strength as

$$\sigma_u + k_1 k_2 \sigma_u = \sigma_u (1 + k_1 k_2)$$

The average strength of the three of the three pillars now becomes

$$\frac{\sigma_u + (\sigma_u + k_1 k_2 \sigma_u) + \sigma_u}{3} = \sigma_u + \frac{k_1 k_2}{3} \sigma_u$$

Taking a row of five pillars the value for the centre pillar becomes

$$\sigma_5 = \sigma_u + k_1 k_2 (\sigma_u) + k_1 k_2 (k_1 k_2 \sigma_u)$$

$$= \sigma_u (1 + k_1 k_2 + (k_1 k_2)^2)$$

Extending this to a wide pillar of $2N - 1$ unit pillars, thus making the centre pillar the N^{th} pillar, the strength of the N^{th} pillar becomes

$$\sigma_N = \sigma_u (1 + k_1 k_2 + (k_1 k_2)^2 \cdots (k_1 k_2)^{N-1})$$

$$= \sigma_u \sum_{r=0}^{N-1} (k_1 k_2)^r$$

N.B. In this analysis we assume $k_1 k_2$ to be constant for ease of calculation and demonstration. In nature this may not be so, as k_1 and k_2 are individually known to vary with stress. However, on first observations they appear to vary inversely and thus, their product varies far less than they do, if it does not in fact remain a constant.

This solution, however, exists only for a wide pillar containing an exact odd number of unit pillars. Values can be calculated for these and then interpolated (see Fig.11d); or we can use a different approach.

This new approach uses the strength value of the unit pillar as the fundamental statement and the rate of increase in strength at the N^{th} pillar as that which occurs over the rest of the wide pillar.



A WIDE PILLAR SUBDIVIDED INTO A ROW OF UNIT PILLARS

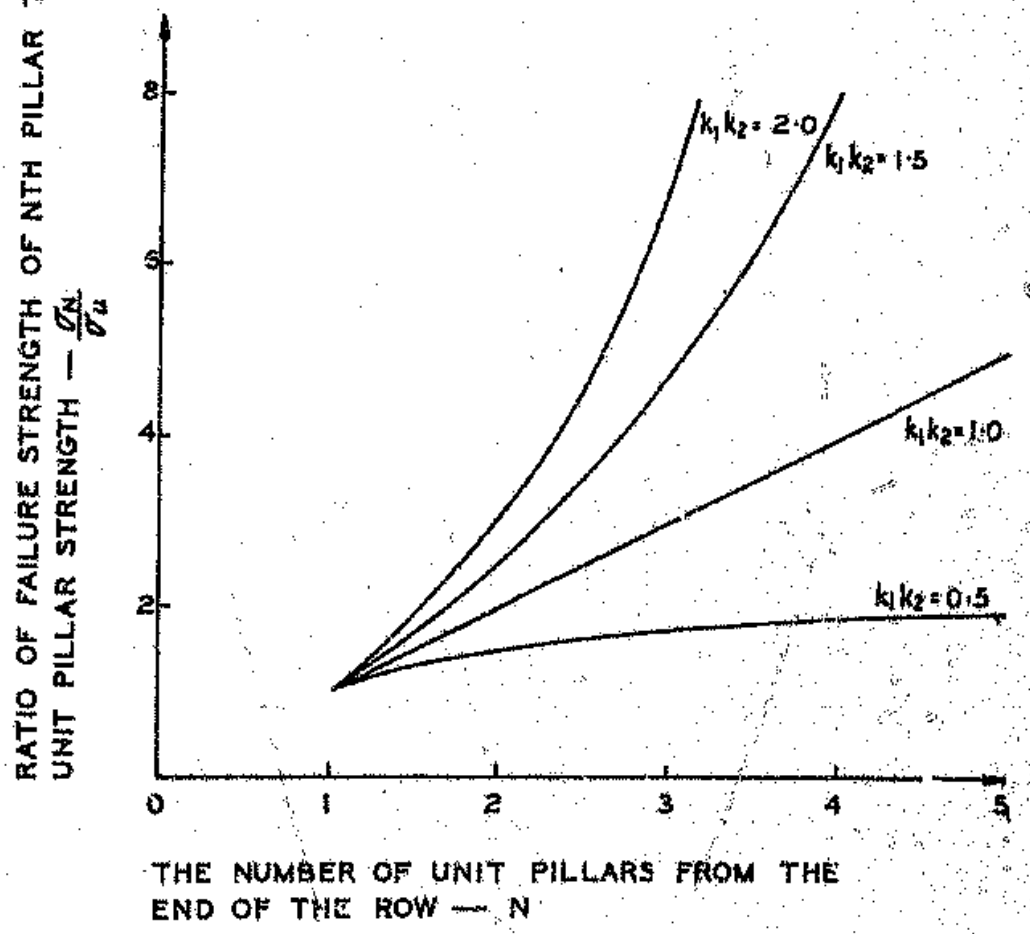


FIGURE 11d. THE STRENGTH INCREASE OF A UNIT PILLAR WITH THE INCREASE IN NUMBER OF UNIT PILLARS FROM THE END OF A ROW OF UNIT PILLARS FOR VARIOUS VALUES OF $k_1 k_2$.

At the N^{th} pillar the slope of the strength curve is the difference between the strength of the $(N+1)^{th}$ pillar and the $(N-1)^{th}$ pillar over the area of the two pillars.

i.e. Slope $= \frac{d\sigma}{dN} \approx \frac{\Delta\sigma}{\Delta N} = \frac{\sigma_{N+1} - \sigma_{N-1}}{2}$

$$= \frac{\sigma_u \left((k_1 k_2)^N + (k_1 k_2)^{N-1}\right)}{2}$$

$$= \frac{\sigma_u (c^N + c^{N-1})}{2}$$

where $c = k_1 k_2$

Taking a pillar of width 2n (thus having symmetry about the centre line at n) and, bearing in mind that the strength of a unit pillar must be σ_u i.e. when $n = \frac{1}{2}$ (i.e. the width to height ratio = 1), $\Delta\sigma$ must = o, the increase is given as

$$\Delta\sigma = \sigma_u \int_{\frac{1}{2}}^{n} \left(\frac{c^n + c^{n-1}}{2} \right) dn$$

Integrating

$$= \sigma_u \left(\frac{c^n + c^{n-1} - c^{\frac{1}{2}} - c^{-\frac{1}{2}}}{2 \log c} \right)$$

Therefore the strength at a point distant n into the pillar is

$$\sigma_n = \sigma_u + \Delta\sigma$$

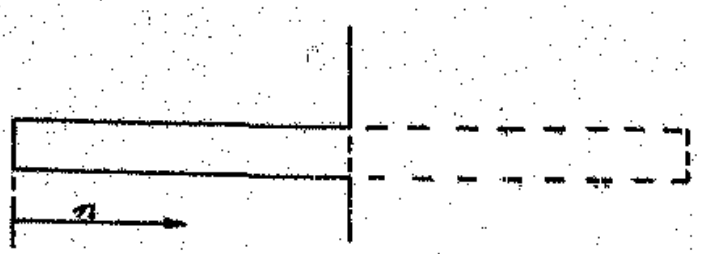
$$= \sigma_u \left(1 + \frac{c^n + c^{n-1} - c^{\frac{1}{2}} - c^{-\frac{1}{2}}}{2 \log c} \right)$$

where $c = k_1 k_2$

(See Fig. 12).

5.6. STRIP PILLAR ANALYSIS

A strip pillar is defined as a pillar which has a length far greater than its width. Ideally the length should be infinite.



CROSS SECTION OF A WIDE PILLAR.

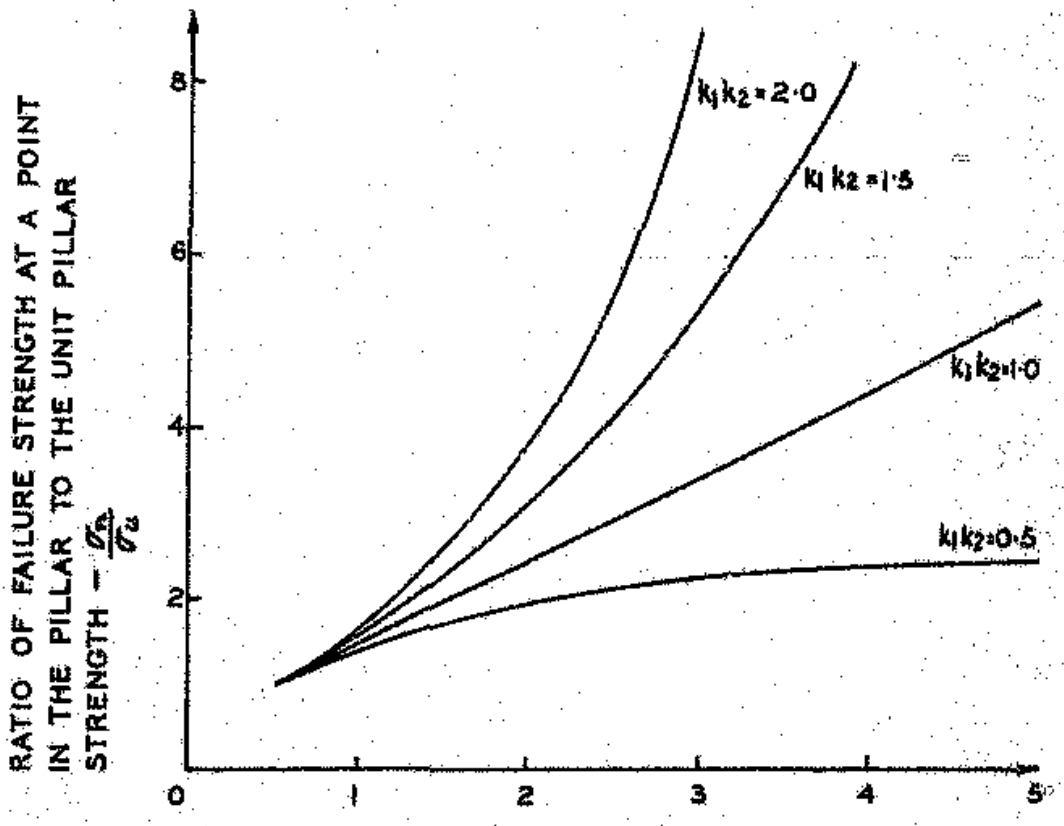


FIGURE 12. THE STRENGTH INCREASE OF A PILLAR TOWARDS ITS CENTRE.

In determining the average strength of a pillar we can use the equations derived in section 5.5 for either the finite element approach, i.e.

$$\sigma_{II} = \sigma_u \sum_{r=o}^{n-1} (k_1 k_2)^r$$

or the continuous rate of increase approach, i.e.

$$\sigma_n = \sigma_u \left(1 + \frac{c^n + c^{n-1} - c^{\frac{1}{2}} - c^{-\frac{1}{2}}}{2 \log c}\right)$$

where $c = k_1 k_2$

5.6. Finite Element Approach

Take a strip pillar of width to height ratio = 3, i.e. the pillar can be subdivided into 3 unit pillars. The strength of the two outer unit pillars is σ_u and that of the centre unit pillar is $\sigma_u(1+k_1k_2)$. Hence the average stress of the pillar

$$\sigma_{av} = \frac{2 \times \sigma_u + 1 \times \sigma_u (1+k_1k_2)}{3}$$

$$= \frac{3\sigma_u + \sigma_u k_1 k_2}{3}$$

$$= \sigma_u \frac{(1+k_1k_2)}{3}$$

Similarly with a strip pillar of width to height ratio = 5, we have the two ultimate unit pillars of strength σ_u, the two penultimate unit pillars of strength $\sigma_u(1+k_1k_2)$ and the centre unit pillar of strength $\sigma_u(1+k_1k_2+(k_1k_2)^2)$ giving an average strength

$$\sigma_{av} = \frac{2\times\sigma_u + 2\times\sigma_u(1+k_1k_2) + 1\times\sigma_u(1+k_1k_2+(k_1k_2)^2)}{5}$$

$$= \frac{5\sigma_u + 3\sigma_u k_1 k_2 + \sigma_u (k_1k_2)^2}{5}$$

$$= \sigma_u \left(1+\frac{3}{5}k_1k_2 + \frac{(k_1k_2)^2}{5}\right)$$

Extending this to the general case of a strip pillar of width to height ratio = R, where R is an odd integer, the average strength becomes,

$$\sigma_{av} = \sigma_u \cdot \left\{ \frac{R}{R} + \frac{(R-2)\,k_1k_2}{R} + \frac{(R-4)(k_1k_2)^2}{R} + \cdots + \frac{(R-(R-1))(k_1k_2)^{\frac{R-1}{2}}}{R} \right\}$$

$$= \sigma_u \sum_{r=0}^{\frac{R-1}{2}} \left(\frac{R-2r}{R}\right) (k_1k_2)^r$$

From this expression values of σ_{av} can be plotted for discreet values of R (R can only be an odd integer). If intermediate values are required, the discreet results obtained can be interpolated by fitting a curve through these points. (See Fig 13).

As a close approximation and for ease of calculation (see Appendix IX), this method is ideal for practical use on the mines as it entails nothing more in understanding than a knowledge of high school mathematics.

5.6. 2. Continuous Rate of Increase Approach

This method entails the use of the continuous rate of increase in strength towards the centre of the pillar. To find the average strength, we integrate the expression for increase of strength and divide by the area. Hence the average strength of a strip pillar is obtained by dividing the total strength of one row of unit pillars across the width by the area which is now the area of one row of unit pillars.

However, the equation must satisfy one boundary condition, i.e. the unit pillar must have a strength of σ_u. This determines

/the

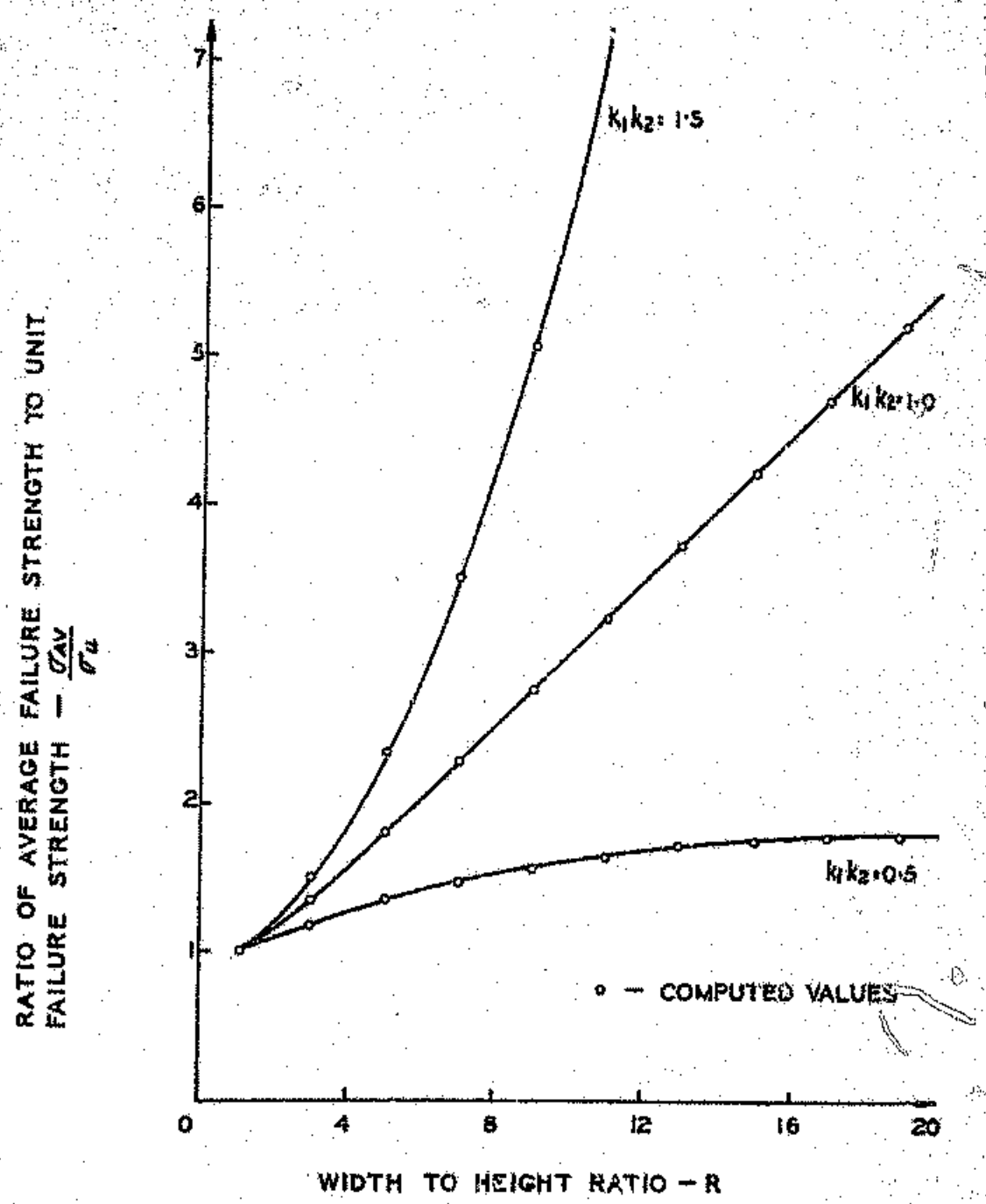


FIGURE 13. THE RELATIONSHIP BETWEEN THE AVERAGE FAILURE STRENGTH AND THE WIDTH TO HEIGHT RATIO OF WIDE STRIP PILLARS FOR VARIOUS k_1k_2 VALUES USING THE FINITE ELEMENT APPROACH.

the limits of intergration. The lower limit becomes $R = \frac{1}{2}$ instead of $R = 0$. As the pillar strength distribution is symmetrical about its centre, the upper limit becomes $\frac{R}{2}$. To find the total strength, the result of the half pillar is doubled.

As the derived strength curve is actually the increase in strength above the value for a unit pillar, σ_u, the total strength will be represented by the sum of the two areas A and B in figs 14a. Mathematically this total area is given by

$$A + B = \sigma_u R + 2 \int_{\frac{1}{2}}^{\frac{R}{2}} \left(\frac{c^n + c^{n-1} - c^{\frac{1}{2}} - c^{-\frac{1}{2}}}{2 \log c}\right) dn$$

where $c = k_1 k_2$

Integrating

$$= \sigma_u R - 2 \left(\frac{c^{\frac{1}{2}} + c^{-\frac{1}{2}}}{2 \log c}\right)\left(\frac{R}{2} - \frac{1}{2}\right) + 2 \left(\frac{c^{\frac{R}{2}} - c^{\frac{1}{2}}}{2 \log^2 c}\right) + 2\left(\frac{c^{\frac{R-1}{2}} - c^{-\frac{1}{2}}}{2 \log^2 c}\right)$$

$$= \sigma_u R - \left(\frac{c^{\frac{1}{2}} + c^{-\frac{1}{2}}}{2 \log c}\right)(R-1) + \left(\frac{c^{\frac{R}{2}} \cdot c^{\frac{1}{2}}}{c \log^2 c}\right)(c+1)$$

Dividing by the area (or width to height ratio R as the length is unity) to find the average strength, σ_{av}, the equation becomes

$$\sigma_{av}/\sigma_u = \frac{A+B}{R} = 1 - \frac{(c^{\frac{1}{2}} + c^{-\frac{1}{2}})(R-1)}{2R \log c} + \frac{(c^{\frac{R}{2}} - c^{\frac{1}{2}})(c+1)}{cR \log^2 c}$$

i.e.

$$\sigma_{av}/\sigma_u = 1 - \frac{(k_1 k_2)^{\frac{1}{2}} + (k_1 k_2)^{-\frac{1}{2}})(R-1)}{2R \log(k_1 k_2)} + \frac{((k_1 k_2)^{\frac{R}{2}} - (k_1 k_2)^{\frac{1}{2}})(k_1 k_2 + 1)}{k_1 k_2 R \log^2(k_1 k_2)}$$

This result is valid for any value of R greater than unity and, being continuous, σ_{av} can be calculated and plotted by computer for any given $k_1 k_2$ (See Fig. 14b and Appendix IV).

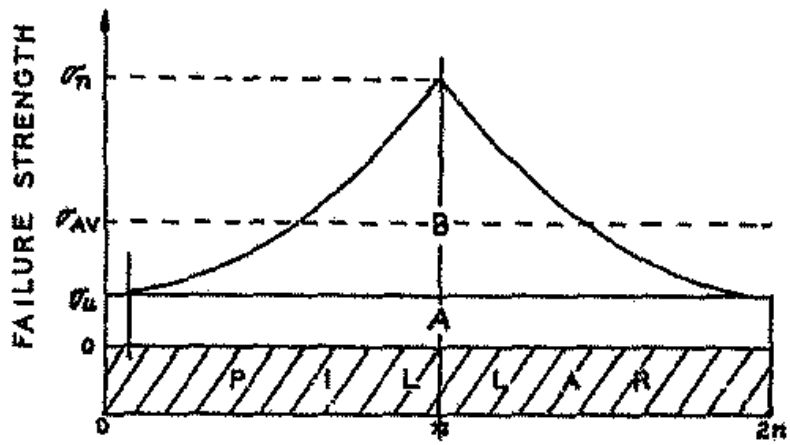


FIGURE 14a. FAILURE STRENGTH DISTRIBUTION OVER A WIDE PILLAR.

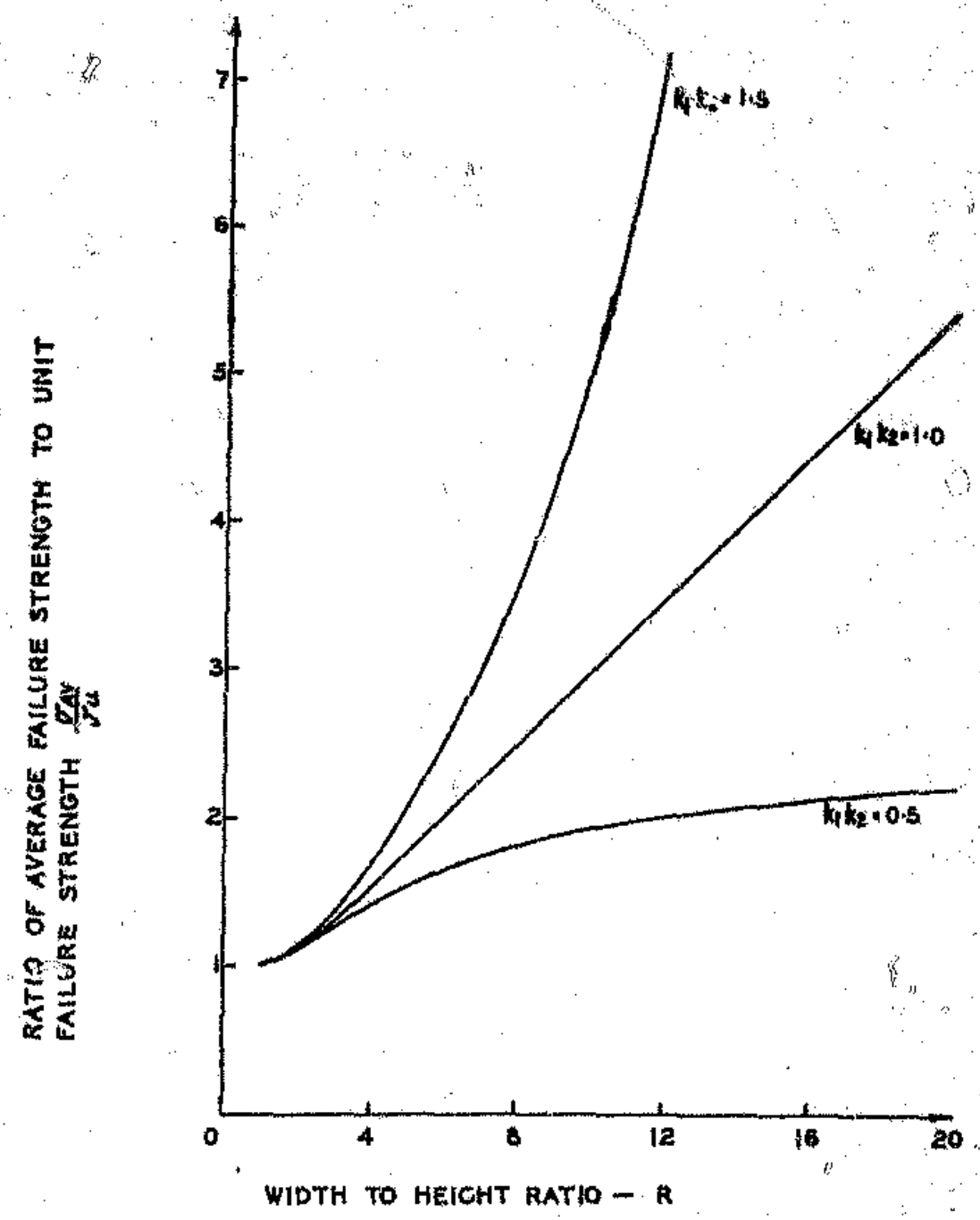


FIGURE 14(b) THE RELATIONSHIP BETWEEN THE AVERAGE FAILURE STRENGTH AND THE WIDTH TO HEIGHT RATIO OF WIDE STRIP PILLARS USING THE CONTINUOUS RATE OF INCREASE APPROACH.

5.6.3. The Comparison of the Finite Element and the Continuous Rate of Increase Approach

In comparing the two approaches (see Appendix V) it is found that, for a value of $k_1 k_2 = 1$, the two sets of results appear identical. This is due to the straight line increase of strength when $k_1 k_2 = 1$ and thus, the approximation over a finite distance in the finite element method becomes exact i.e. the median coincides with the mean over any element. However, when $k_1 k_2$ is not equal to unity, a slight error occurs due to a differential increase in strength. When $k_1 k_2$ is greater than unity, the curve of the continuous strength increase is concave up (see Fig 14b) and therefore, the results of the finite element approach are in excess of the results of the continuous approach. If $k_1 k_2$ is less than unity the continuous curve is concave down and the results of the finite element approach are below the results of the continuous approach. The further $k_1 k_2$ deviates from unity and the greater the value of R, the greater the deviation becomes.

Therefore, the finite element approach can be used if $k_1 k_2$ lies close to unity (say $0.5 < k_1 k_2 < 1.5$) and R is not too large (say $R < 10$).

5.7. SQUARE PILLAR ANALYSIS

A square pillar is defined as a pillar which has its length equal to its width.

In the geometry of its shape, the square pillar lends itself ideally to the finite element approach for the calculation of its strength. The ease of division into square elements of unit

/size

size and their summation, eliminates the highly complex mathematics which is entailed in attempting to provide a strength distribution surface by using the continuous rate of increase approach.

Certain approximations in the finite element approach must be made to calculate the strength of square pillars. The approximations induce errors opposite in sign to those inherent in the finite element method. The deviation from reality is therefore less than that in the strip pillar.

The application of the finite element method requires that the wide pillar must be able to be divided up exactly into unit pillars with a single unit pillar in the centre. Therefore the width of the wide pillar must be 2N+1 unit pillars with the N^{th} pillar in the centre. The approximation made is that all unit pillars in the outer row have the same strength, viz, that of the unit pillar σ_0. All pillars in the penultimate row have the same strength, viz. slightly greater than the previous row, etc, to the N^{th} row, which happens to be the centre unit pillar. The strengths of all these unit pillars are then summed and the result divided by the area to give the average strength.

Verification of this approximation is given in Appendix III. The error in assuming all unit pillars in a row to be of equal strength is about 10% compared to the 150% increase in strength between rows. This makes the pillar 10% stronger than it is calculated to be and thus cuts down the variable error incurred in using the finite element approach.

To illustrate the method described above consider a pillar of width to height ratio = 3, i.e. an outer row of unit pillars with the same strength σ_u, and a centre unit pillar with increased strength $\sigma_u + k_1k_2\sigma_u$. There are eight unit pillars in the outer row and one in the centre (see Fig. 15a) giving the average strength

$$\sigma_{av} = \frac{8x\sigma_u + 1x(\sigma_u + k_1k_2\sigma_u)}{9}$$

$$= \frac{9\sigma_u + k_1k_2\sigma_u}{9}$$

$$= \sigma_u(1 + \frac{k_1k_2}{9})$$

Now consider a wide pillar of width to height ratio = 5. There sixteen unit pillars of strength σ_u in the outer row, eight of strength $\sigma_u(1+k_1k_2)$ in the second row and the centre unit pillar of strength $\sigma_u(1+k_1k_2+(k_1k_2)^2)$, (See Fig 15b).giving the average strength

$$\sigma_{av} = \frac{16x\sigma_u + 8x\sigma_u(1+k_1k_2) + \sigma_u(1+k_1k_2+(k_1k_2)^2)}{25}$$

$$= \frac{25\sigma_u + 9\sigma_uk_1k_2 + \sigma_u(k_1k_2)^2}{25}$$

$$= \sigma_u(1+\frac{9}{25}k_1k_2+\frac{1}{25}(k_1k_2)^2)$$

Extending this to the general case of a wide pillar of width to height ratio = R (where R is an odd integer)

$$\sigma_{av} = \sigma_u\left(R^2 + (R-2)^2k_1k_2 + \cdots + (R-(R-1))^2(k_1k_2)^{\frac{R-1}{2}}\right)$$

$$= \sigma_u \sum_{r=0}^{\frac{R-1}{2}} \left(\frac{R-2r}{R}\right)^2 (k_1k_2)^r$$

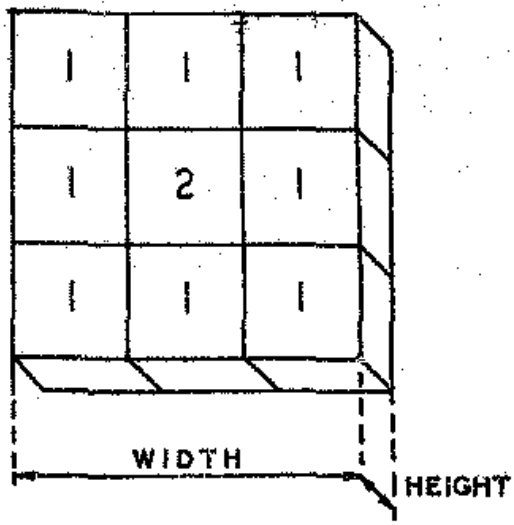


FIGURE 15a. ISOMETRIC VIEW OF A SQUARE WIDE PILLAR OF R=3 SUBDIVIDED INTO UNIT PILLARS WITH ASSUMED LIKE STRENGTHS INDICATED BY LIKE NUMBERS.

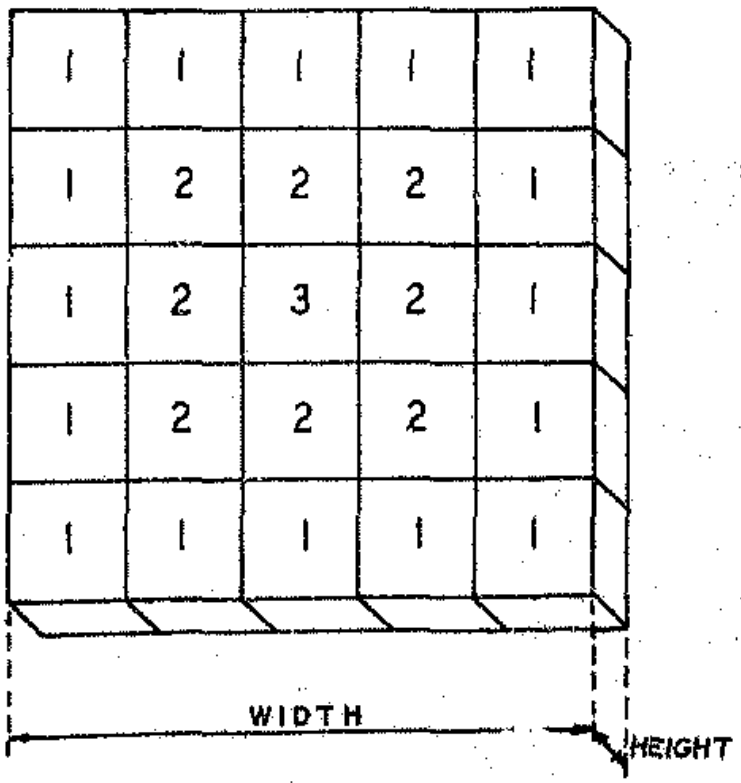


FIGURE 15b. ISOMETRIC VIEW OF A SQUARE WIDE PILLAR OF R=5 SUBDIVIDED INTO UNIT PILLARS WITH ASSUMED LIKE STRENGTHS INDICATED BY LIKE NUMBERS.

From this expression values of σ_{av} can be plotted for discrete odd integer values of R and the intermediate values can be obtained by interpolation. ~~(See Fig 15c).~~

If one wishes to avoid interpolation and prefers a continuous expression, the discreet summation can be approximated by the function

$$\sigma_{av} = \sigma_u \left[\overline{1+\frac{c}{R^2}}^{\frac{R}{2}} \left\{ \left(\frac{8}{\log^3 c} \right) - \frac{c^{\frac{1}{2}}}{R^2} \left\{ \frac{(R-1)^2}{\log c} + \frac{4(R-1)}{\log^2 c} + \frac{8}{\log^3 c} \right\} \right\} \right]$$

where $c = k_1 k_2$

(See Appendix VI for the proof)

This expression can be computerised, calculated and plotted for all values of R greater than unity.

5.8. CIRCULAR PILLAR ANALYSIS

A circular pillar is defined as a pillar which has circular horizontal cross-section, i.e. it is an upright cylinder.

As opposed to the square pillar, the circular pillar, by the very essence of its shape, lends itself ideally to the continuous rate of increase approach in determining the average strength of the pillar. The division of a circle into square elements proves problematical. However, if one wishes to calculate the average strength of a pillar simply, the equating of a square pillar to its inscribed circular pillar serves as a good first approximation.

Again, as with the strip pillar, the expression for the continuous rate of increase of strength is used. This expression is integrated to obtain the area below the curve (area B in Fig 16a),

/rotated

From this expression values of σ_{av} can be plotted for discrete odd integer values of R and the intermediate values can be obtained by interpolation. ~~(See Fig 15c).~~

If one wishes to avoid interpolation and prefers a continuous expression, the discreet summation can be approximated by the function

$$\sigma_{av} = \sigma_u \left[1+\frac{c}{R^2}\left(\frac{8}{\log^3 c}\right) - \frac{1}{R^2}\left\{\frac{(R-1)^2}{\log c} + \frac{4(R-1)}{\log^2 c} + \frac{8}{\log^3 c}\right\}^{\frac{R}{2}}\right]$$

where $c = k_1 k_2$

(See Appendix VI for the proof)

This expression can be computerised, calculated and plotted for all values of R greater than unity.

5.8. CIRCULAR PILLAR ANALYSIS

A circular pillar is defined as a pillar which has circular horizontal cross-section, i.e. it is an upright cylinder.

As opposed to the square pillar, the circular pillar, by the very essence of its shape, lends itself ideally to the continuous rate of increase approach in determining the average strength of the pillar. The division of a circle into square elements proves problematical. However, if one wishes to calculate the average strength of a pillar simply, the equating of a square pillar to its inscribed circular pillar serves as a good first approximation.

Again, as with the strip pillar, the expression for the continuous rate of increase of strength is used. This expression is integrated to obtain the area below the curve (area B in Fig 16a),

/rotated

rotated about the centre-line of the pillar to obtain the solid of revolution below the strength surface, then added to the unity cylinder generated by area A in fig. 16 a and, finally, divided by the cross-sectional area of the pillar to obtain the average strength.

In fig. 16b the strength increase curve f(n) is shown with σ_n as the ordinate axis and n as the abscissa. Now let the centre-line of the pillar, i.e. distant radius (r) into the pillar, become the new σ_r axis, about which the strength curve will be revolved, thus producing the strength surface above a circular pillar of radius r. Due to the change of axis, the n- axis becomes the x- axis. As the part of the curve that is to be used, is to the left of the x- axis, for ease of calculation the x- axis operates in the opposite direction to that of the n- axis.

Hence $x = r - n$

or $n = r - x$

The boundary condition that is imposed is that, when the diameter (or width) to height is unity, the strength is that of a unit pillar σ_u. Hence the lower limit of integration will be $x = 0$, and the upper limit will be $x = r - \frac{1}{2}$.

Mathematically the above is expressed as:-

The change of axis results in the change in strength function

$$f(n) = f(r-x)$$

which gives

$$= \frac{c^{r-x} + c^{r-x-1} - c^{\frac{1}{2}} - c^{-\frac{1}{2}}}{2 \log c}$$

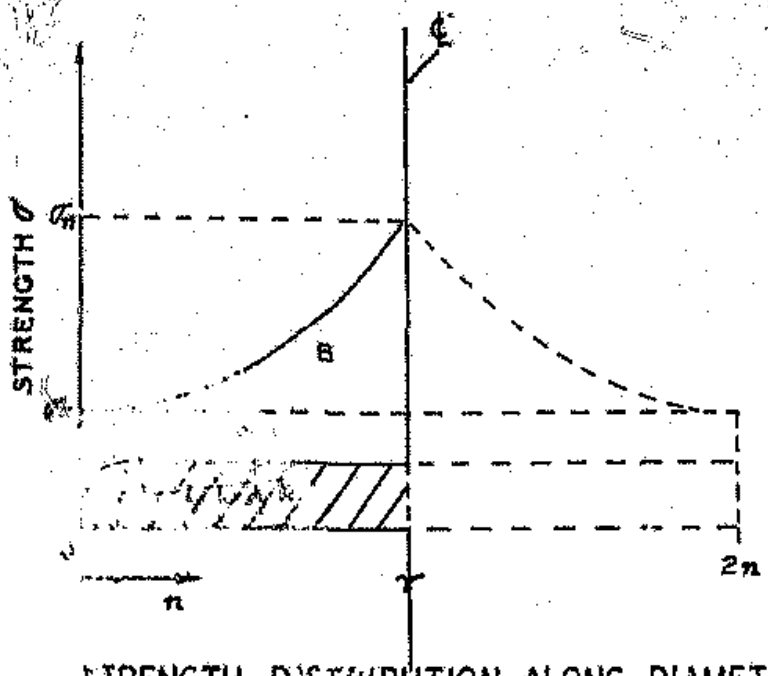


FIGURE 16a. STRENGTH DISTRIBUTION ALONG DIAMETER OF A CIRCULAR WIDE PILLAR.

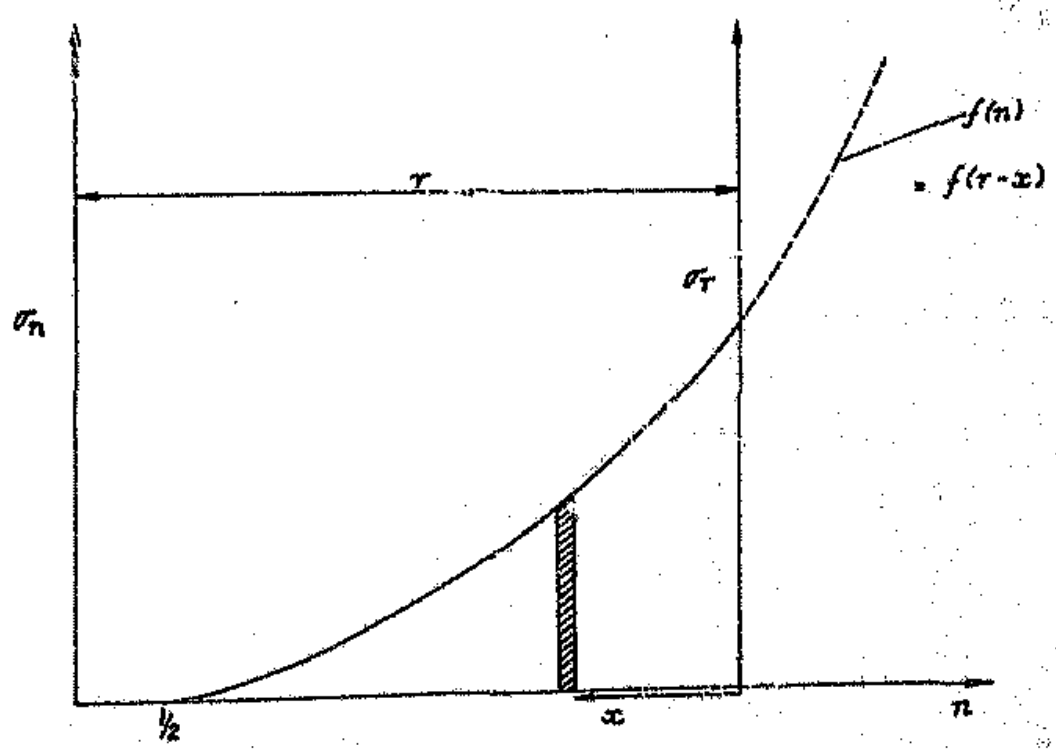


FIGURE 16b. MATHEMATICAL TECHNIQUE FOR FINDING AVERAGE STRENGTH OF A CIRCULAR WIDE PILLAR FOR VARYING RADIUS.

To find the volume generated by area B in fig. 16a

$$\text{Volume B} = \int_0^{r-\frac{1}{2}} 2\pi x f(r-x)\,dx$$

$$= \frac{2\pi}{2\log c}\int_0^{r-\frac{1}{2}} (xc^{r-x} + xc^{r-x-1} - xc^{\frac{1}{2}} - xc^{-\frac{1}{2}})\,dx$$

$$= \frac{\pi}{\log c}\left[\frac{-xc^{r-x}}{\log c} - \frac{c^{r-x}}{\log^2 c} - \frac{xc^{r-x-1}}{\log c} - \frac{c^{r-x-1}}{\log^2 c} - \frac{x^2 c^{\frac{1}{2}}}{2} - \frac{xc^{-\frac{1}{2}}}{2}\right]_0^{r-\frac{1}{2}}$$

$$= \frac{\pi}{\log c}\left[\frac{c^r + c^{r-1}}{\log^2 c} - (c^{\frac{1}{2}} + c^{-\frac{1}{2}})\frac{(r-\frac{1}{2})^2}{2} + \frac{r-\frac{1}{2}}{\log c} + \frac{1}{\log^2 c}\right]$$

The volume generated by area A of fig. 16a

$$\text{Volume A} = \pi r^2$$

Dividing the sum of the volumes by the cross-sectional area gives the average strength of the pillar.

$$\frac{\sigma_{AV}}{\sigma_u} = \frac{\text{Vol A + Vol B}}{\pi r^2}$$

$$= 1 + \frac{c^r + c^{r-1}}{r^2 \log^3 c} - \frac{c^{\frac{1}{2}} - c^{-\frac{1}{2}}}{r^2}\,\frac{(r-\frac{1}{2})^2}{2\log c} + \frac{r-\frac{1}{2}}{\log^2 c} + \frac{1}{\log^3 c}$$

where $c = k_1 k_2$

This result is valid for any value of R greater than unity (i.e. $r > \frac{1}{2}$) and, being continuous $\frac{\sigma_{AV}}{\sigma_u}$ can be calculated and plotted for R, given $k_1 k_2$ (see fig 16c).

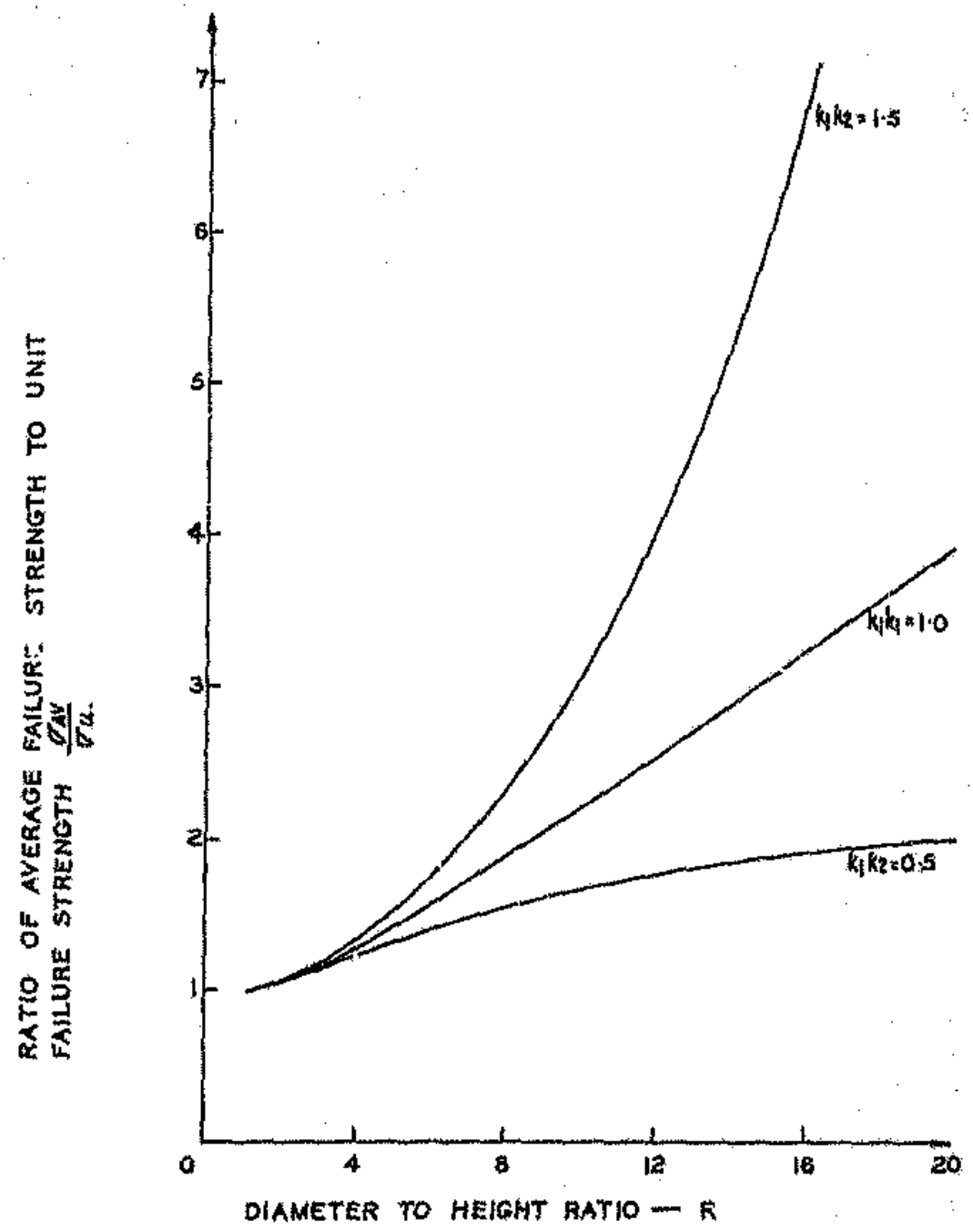


FIGURE 16c. THE RELATIONSHIP BETWEEN THE AVERAGE FAILURE STRENGTH AND THE WIDTH TO HEIGHT RATIO OF WIDE CIRCULAR PILLARS.

CHAPTER 6

LABORATORY INVESTIGATION

6.1 Description of Material for Laboratory Tests

Laboratory experiments were conducted on reddish brown sandstone of the Karroo System from Warmbaths, Northern Transvaal, to find its size-strength relationship. It is a fine (less than 1mm) and even grained material and behaved homogeneously and isotropically. X-ray and microscopic studies revealed no preferential direction of the crystallographic axes.

The open pore structure facilitated the attaining of a 100% saturation. For testing, this uniform standard, with respect to the moisture content, eliminated it as a variable parameter.

The sandstone was able to be easily machined with a diamond saw and therefore a large number of specimens could be cut in a short time. Due to grain size the dimensional tolerance of the specimens was relatively small. The fine grain size of specimens was comparable to, say, conglomerates in actual mining pillars.

From the graphical stress/strain relationship it was found that the rock had a linear elastic behaviour.

6.2 Method of Testing Rock Specimens

6.2. 1. Preparation of Specimens

The sandstone for specimens was supplied in slabs of various thicknesses, viz. ½", ¾", 1", 2", 4". In the series of tests conducted on square blocks with varying width to height ratios, the blocks were cut with 12"

/diameter.....

diameter Diamont Boart diamond saw. The specimen faces which were to be in contact with the pressure plattens, were ground on a lapping disc with abrasive powder of the type "A 150 silicon carbide and alumious oxide".

After preparation the blocks were soaked in water to attain a 100% saturation. The soaking times to saturation and the drying times for the different specimen sizes are given in Appendix VII.

To be well on the safe side, all specimens were soaked for at least 1 day. The 2" blocks were soaked for 3 days.

Before testing the blocks were measured to .001" and tested for parallelity of top and bottom surface.

6.2.2. The Testing Procedure to determine the Specimen Failure Strength

Tests were conducted in a 200 ton Amsler Compression Machine, Type 200 DB 76. The pressure plates were mounted on spherical seats to ensure vertical loading. Two hardened steel plattens were used between the machine pressure plates and specimen to avoid damage to the pressure plates. A second set of smaller spherical seats were used for tests on small specimens. The crosshead was lowered on to the specimen, an initial load of 5,000 lbs was applied, and thereafter the load was increased at a steady rate of about 1000 p.s.i. per second.

Two dial gauges were fitted diagonally across the pressure plates, to check on even loading and to measure strain to .0001". The specimens were tested to destruction. Strain readings at definite load values, corresponding to the load at the first

audible crack and the failed load were taken and the mode of failure was noted. For some specimens a continuous graph of load versus strain was recorded.

6.3. INFLUENCE OF VARIOUS FACTORS ON THE FAILURE STRENGTH

Hoek[20] and Wiid[19] describe the influence of the following factors on the failure strength of brittle solids:

6.3.1. The Isotropy of the material

If the strain and the uniaxial compressive strength of specimens are invariant with respect to its bedding planes, then it is macroscopically isotropic. For the sandstone specimens no preferred failure or strain direction was found.

6.3.2. Griffith cracks

The inherent cracks in the rock are expected to be closed even at no load. If they are open it would be expected that the stress/strain curve should be non-linear for low stress values. As the curves for sandstone are linear it implies that only the modified Griffiths theory of failure has to be considered.

6.3.3. Vapour pressure

The internal vapour pressure on the crack surfaces within a rock under stress creates a pressure system which lowers or increases the strength of the material. To eliminate vapour pressure effects the specimens were tested at 100% saturation.

6.3.4. Temperature

Temperature affects the rock strength of rock at very low temperatures in the same sense as it effects steel to cause low temperature brittleness, and at high temperatures when the constituents

approach their melting points. The series of tests were conducted at room temperature, thus eliminating the effects of temperature.

6.3.3. Rate of Loading

The strength of rock properties is time dependent. The strength may vary as much as 20% for loads applied in milliseconds or over years. This loading rate for the present series of tests was constant and therefore the effects of the loading rate are not considered.

6.3.6. The Effect of Interfaces

The effect of using a model made up of slices instead of a solid specimens was investigated by determining the failure strength of specimens made up with interfaces having

1. No filling
2. Plaster of Paris filling
3. Araldite glue filling

It was found that the sliced specimens were very much weaker than the solid ones with or without filling. (See Appendix VIII).

Therefore, tests were made on solid specimens only. The effect of the interfaces between specimens and pressure plattens was investigated by comparing results obtained by using metal plattens and sandstone plattens. The limited number of tests indicated no significant difference. (See Appendix IX).

Therefore, testing was conducted with metal plattens only which resisted wear and facilitated a standardised testing procedure.

CHAPTER 7

RESULTS

7.1 OBSERVATION OF THE MODE OF FAILURE

The graphical record of the stress / strain relationship of laboratory size sandstone specimens shown in fig 17(a) is linear from the no-stress condition to the failure condition. The specimens with a large width to height ratio tend to scale around the perimeter prior to failure, leaving a solid core in the centre as shown in fig 17 (b). In plan view, diagonal cracks form from the corners towards the centre until they reach the solid core. These cracks could be caused by the outward movement of rock in expanding laterally. Around the core, which tends to be circular in shape, a series of concentric circular cracks or failure planes exists. These failure planes could be the result of the strength increase towards the centre with first the sidewalls scaling off and then a succession of scaling, until the remaining portion of the pillar, the core, can no longer carry the increased load, resulting in sudden failure.

The blocks of low width to height ratio tend to show failure planes, typical of active shear, forming a cone or a section thereof.(see fig 17 (c)). These appear to be consistent with the conventional mode of coal pillar failure in practice. An interesting aspect of this cone type failure is that on close examination, it is not a straight line fracture but a series of continuous steps (see fig 17(d)). This could be explained either a) by the fact that the grains themselves do not shear, but that shearing takes place along their boundaries, or b) that is is a series of Griffith cracks propagating.

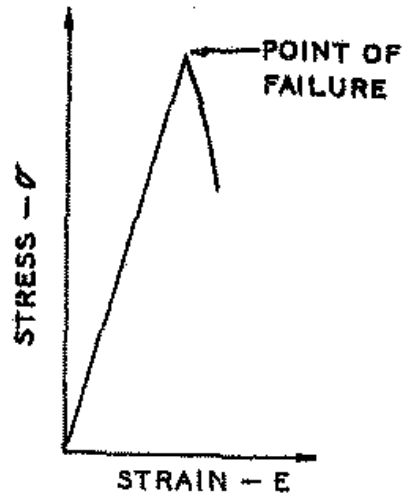


FIGURE 17a. STRESS-STRAIN DIAGRAM OF SANDSTONE

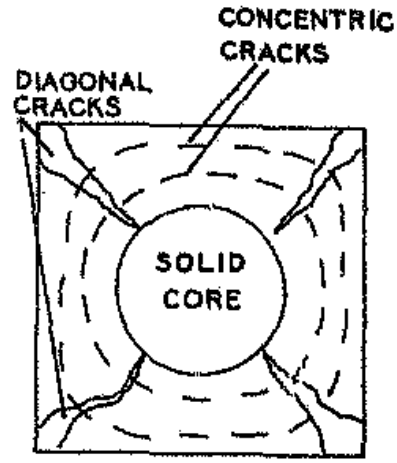


FIGURE 17b. PLAN VIEW OF A SANDSTONE MODEL OF LARGE (>4) WIDTH TO HEIGHT RATIO SHOWING DIAGONAL CRACKS, CONCENTRIC CRACKS AND SOLID CORE PRIOR TO ULTIMATE FAILURE.

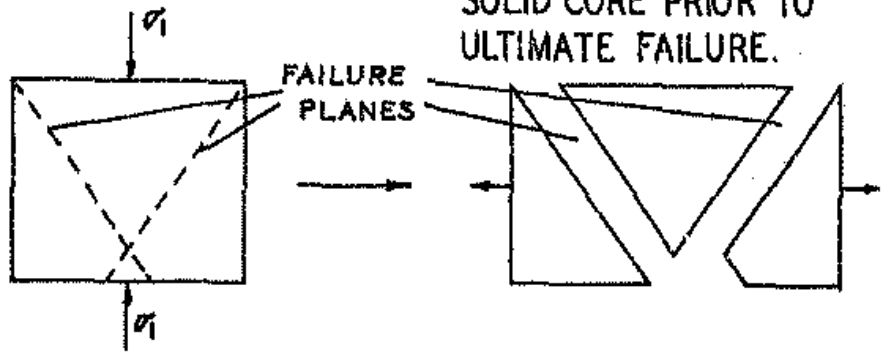


FIGURE 17c. SIDE ELEVATION OF A SANDSTONE MODEL OF LOW WIDTH TO HEIGHT RATIO SHOWING THE DEVELOPMENT OF FAILURE PLANES.



FIGURE 17d. SIDE ELEVATION OF A SANDSTONE MODEL AFTER FAILURE SHOWING THE FAILURE PLANE TO CONSIST OF A SERIES OF STEP FRACTURES.

7.2. DEFINITION OF FAILURE

Violent failure facilitates the determination of the precise point of failure. It provides a good definition of failure in that a large amount of strain is experienced before the system is able to carry load once more. This point of failure is clearly shown on the stress/strain diagram as that point at which a large increase in strain with regard to stress is initiated.

When failure is non-violent and occurs by deterioration and disintegration of the specimen, the point of failure is less easy to establish. Under these conditions, the point of failure can be defined as that point at which the maximum load can be carried.

Therefore, the general definition of failure is that failure occurs at the stress represented by the point on the stress/strain curve where the slope changes from positive to negative.

CHAPTER 8

DISCUSSION OF RESULTS

8.1 LABORATORY TESTS

A series of tests were conducted in the laboratory on sandstone square pillar models of constant height and varying width, to give a range of width to height ratios (R) for $1.8 \leq R \leq 6.7$. Models outside this range could not be tested due to the limits of the testing machine. Tests on smaller models could not be sufficiently controlled for accuracy of results due to possible off-centre loading and small load readings. Larger models were beyond the test machine's capacity. To change the test machine to increase the range would mean that the testing method is changed thus providing a whole new set of parameters for which provision must be made. Due to the difficulty in recognising these parameters, doubt is cast on the validity in extending the results in this manner.

The ultimate strengths for the different width to height ratios were calculated. A graph of this relationship was drawn and a computer-calculated polynomial best fit superimposed (see Fig 18a).

From work by Wiid[19] on similar sandstone, values were obtained of k_1 and k_2 of 8.5 and .15 respectively, giving $k_1\ k_2$ a value of 1.5. A family of curves for $k_1\ k_2$ equal to 1.3, 1.5 and 1.7 is compared to the results (see Fig. 18b). It can be seen that this provides a very good fit.

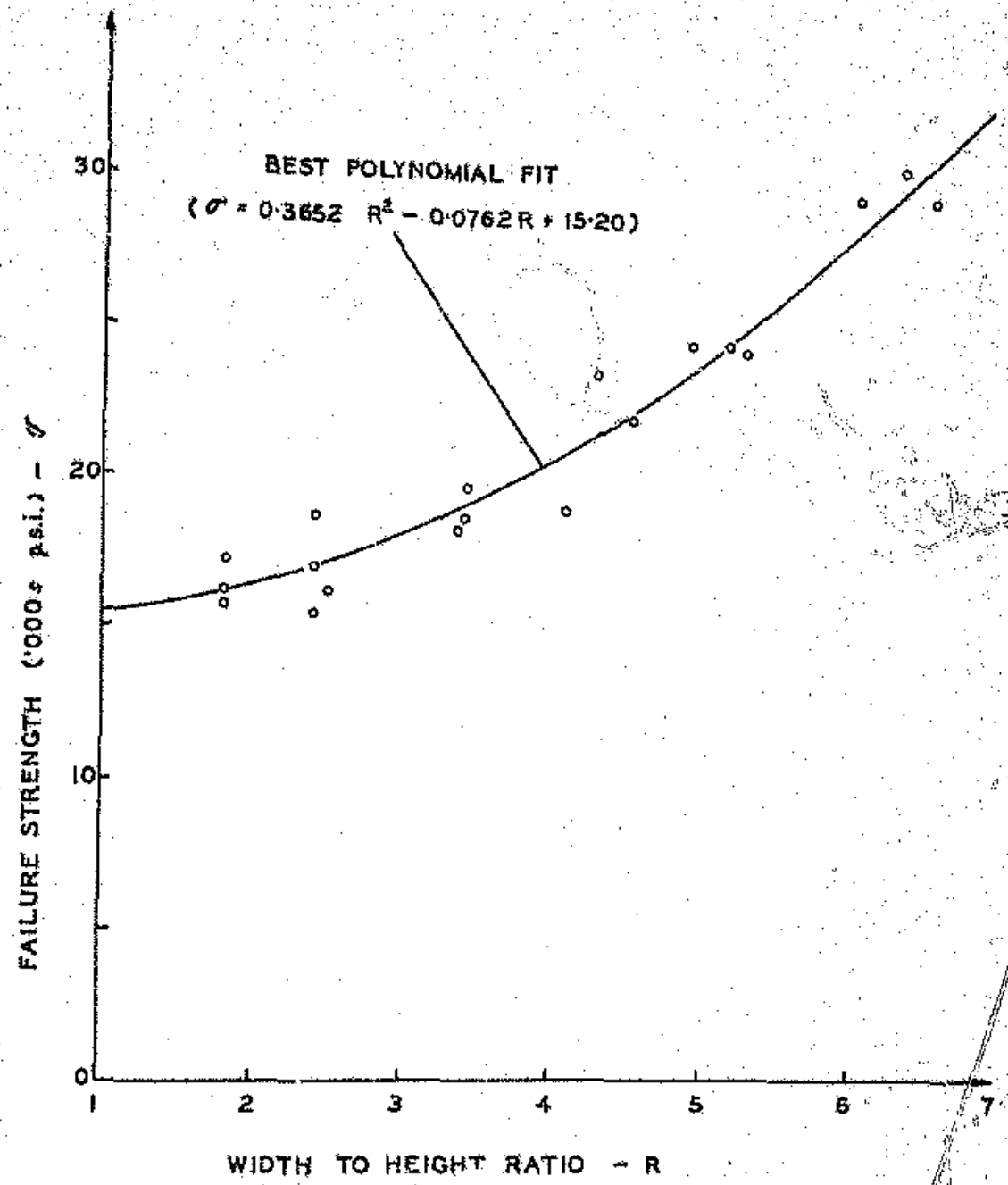


FIGURE 18a. RESULTS OF COMPRESSIVE TESTS ON SANDSTONE SQUARE PILLAR MODELS OF HEIGHT ½" SHOWING THE POLYNOMIAL CURVE OF BEST FIT.

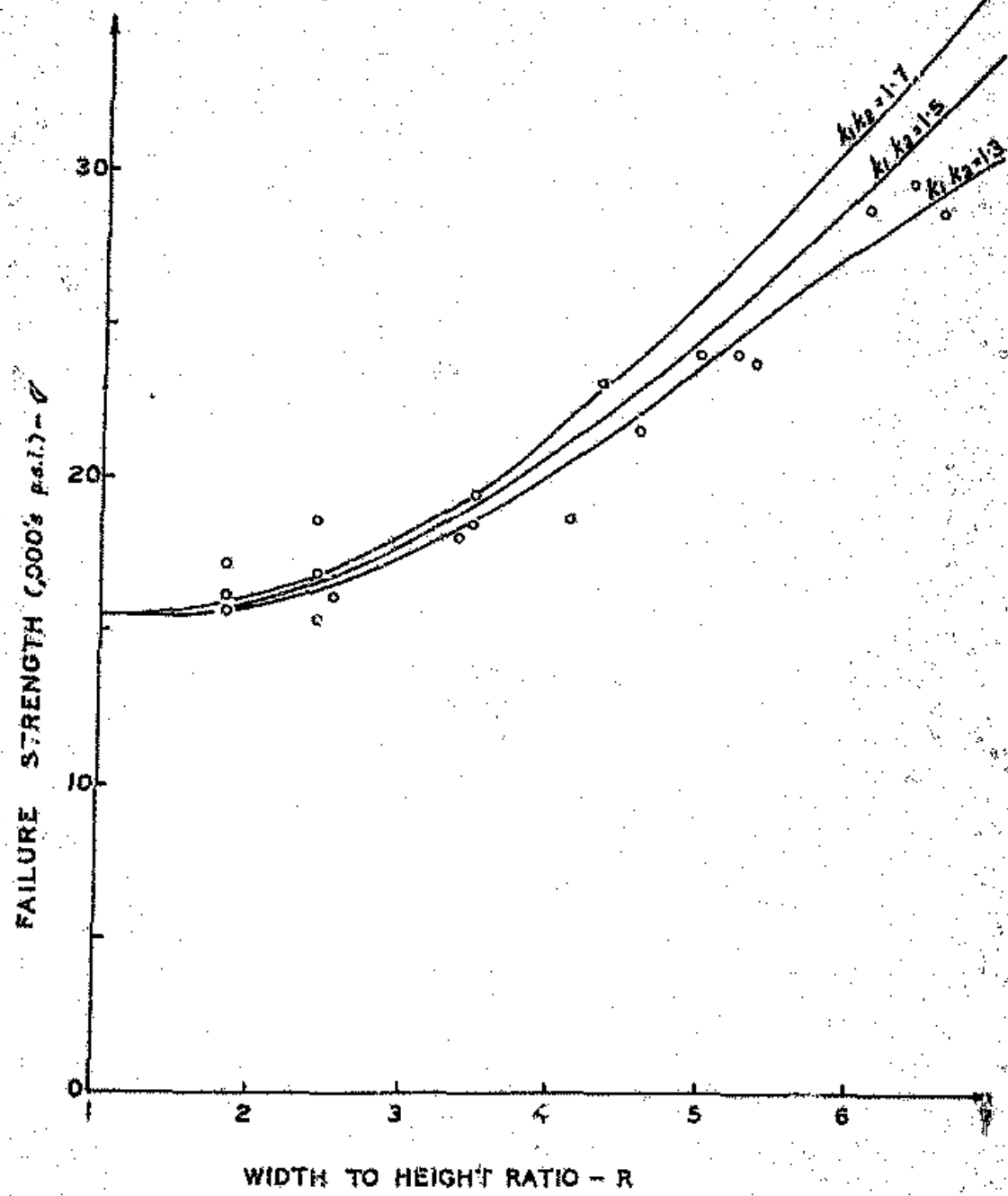


FIGURE 18b. RESULTS OF COMPRESSIVE TESTS ON SANDSTONE SQUARE PILLAR MODELS OF HEIGHT ½" SHOWING THEORETICAL CURVES FOR $k_1 k_2 = 1{\cdot}3, 1{\cdot}5, 1{\cdot}7$ SUPERIMPOSED.

What is more important though, is that the trend of the theoretically derived curve, i.e. concave up, corresponds to that of the results. This accelerating increase in strength with constantly increasing width to height ratio is peculiar to this theory and is a feature for which no other theory has provided. The logical extension of this characteristic is that at a not so very great width to height ratio, a large amount of load can be carried - in practice approaching infinity.

The observation during testing of the tendency for the material to fail from the perimeter of the pillar towards the centre at substantial increases of load, verify the concept of the strength increasing towards the centre. This is also observed in mining practise in the scaling effect of pillars.

8.2. COMPARISON WITH PREVIOUS THEORIES

The theories stated in section 4 of this dissertation can be classed into two categories:-

(a). the power function formulae.

(b). the linear relationship.

By keeping the height constant, as was done in the laboratory tests, the power function theories proposed by Greenwald et al[14], Steart[15], Salamon and Munro[16] and Bieniawski[17] can be reduced from

$$\sigma = k\, w^{a} h^{b}$$

to

$$\sigma = k \left(\frac{w}{h}\right)^{a} h^{b+a}$$

$$= k\, R^{a} h^{b+a}$$

$$= K R^{a}$$

It can be seen that when R = 1, $R^a = 1$ and therefore K corresponds to the strength value of the unit pillar. (σ_u). i.e. the equation becomes $\sigma = \sigma_u R^a$

The corresponding values of a for the theories can be summarised as follows:

	a
Greenwald et al	0.50
Steart	0.50
Salamon and Munro	0.46
Bieniawski	0.16

The limited range of observations necessitates a small scatter in results to obtain precise formulae. Alternatively, many observations have to be made. In fact only one formulator tested many specimens over a sufficient range of sizes. (Salamon and Munro). The extrapolation of the other formulae contains a serious risk of misleading deductions.

From the above table it can be seen that for each theory there exists a single strength - width to height ratio curve. In the cases of Greenwald, Steart and Bieniawski, this is due to the fact that the formulae were empirically derived from tests on a single coal type. In the case of Salamon and Munro it is due to the fact that the formula was empirically derived from the statistical mean of many varied coal types. No doubt that the value of "a" would change with a change of material. Hence, these formulae only have use in determining the strength of material of the same type from which they were derived.

From the graphical comparison of the theories (see Fig.19a) it is seen that in all but the case of Salamon and Munro, the

/formulae

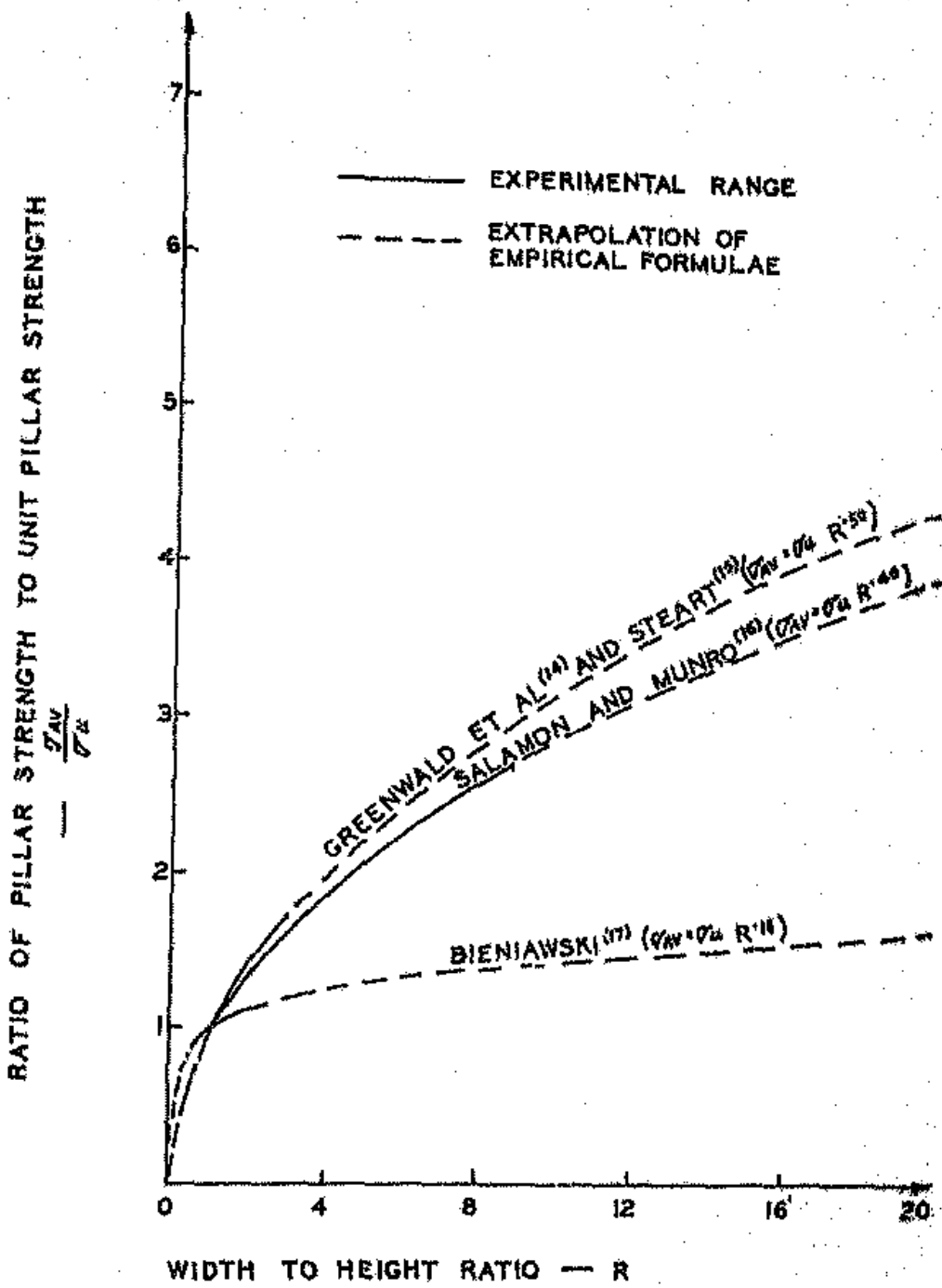


FIGURE 19a. COMPARISON OF SOME PREVIOUS PILLAR STRENGTH THEORIES (THE "POWER FUNCTION FORMULAE") KEEPING THE HEIGHT CONSTANT AND VARYING THE WIDTH TO PRODUCE VARIOUS VALUES OF WIDTH TO HEIGHT RATIO.

formulae have been derived by tests over a limited region and then extrapolated to apply to practical mining conditions. It is also observed that over such a limited range the results would have to have remarkably small deviation from the strength curve, something which is not readily found in nature, or else have taken a large number of readings, which only one formulator did, to produce a formula so precise; more especially so, when one wishes to extrapolate.

In comparing the power function formulae with the derived square pillar formula postulated in this dissertation (see Fig.19b) it is seen that, although the curves are valid over a limited region of $k_1 k_2$ values, they differ greatly on extrapolation. The major difference is that while the derived formula is concave up, the power function formulae are concave down. The reason for this is that the power function formula inherently assumes the strength curve to pass through the origin.

The derived formula makes no attempt to state what happens as the width to height ratio approaches zero, as it is defined only for the ratio above unity. It only indicates that it does not pass through the origin, which bears up well with experimental work.

In addition the experimental results on sandstone (see Fig 18a) show a distinct tendency to obey an accelerating increase in strength with a constant increase in the width to height ratio i.e. a strength curve which is concave up.

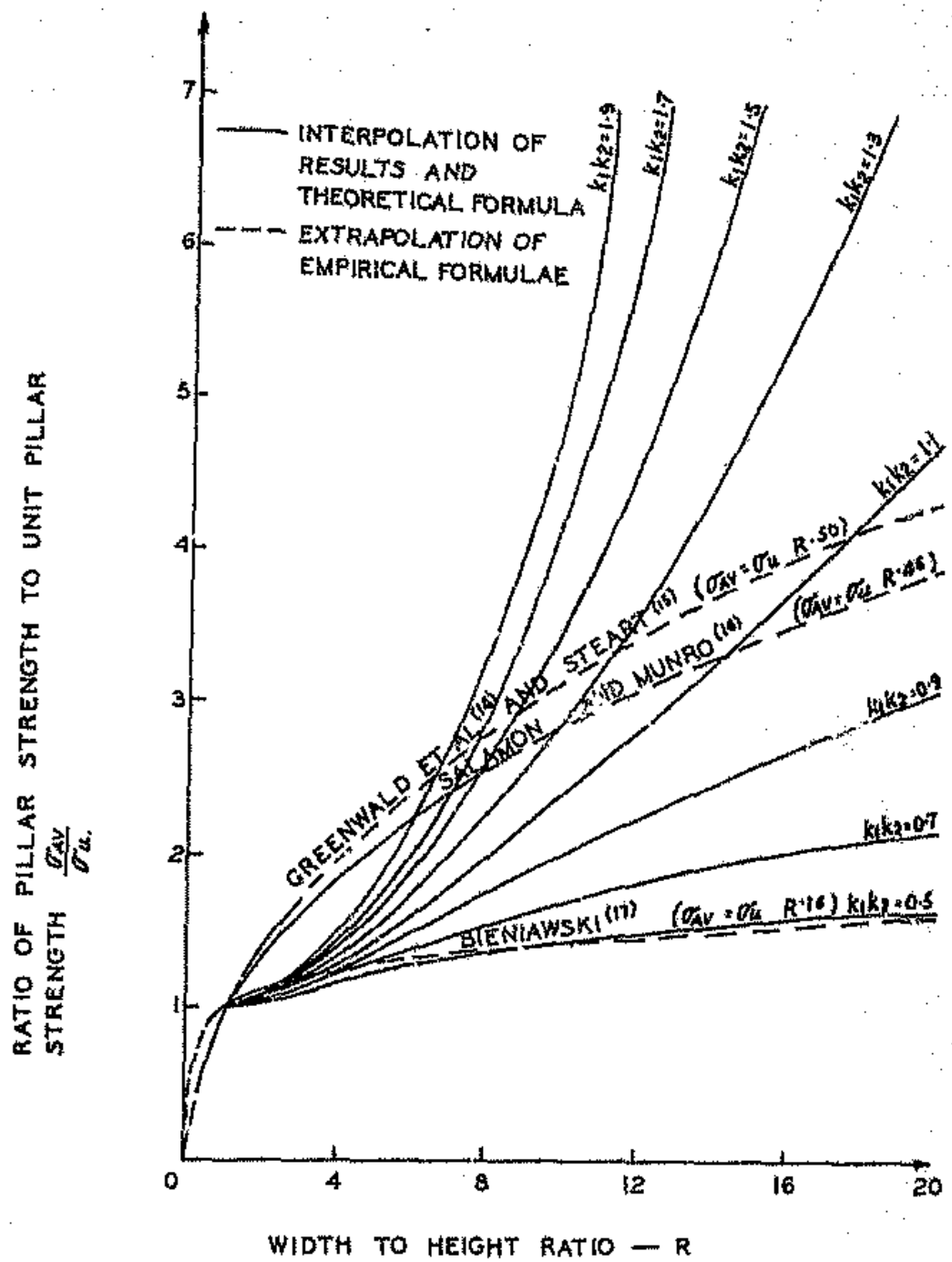


FIGURE 19b. COMPARISON OF THE "POWER FUNCTION FORMULAE" TO THE POSTULATED THEORETICAL RELATIONSHIP.

In a later publication Bieniawski[18] proposes a linear relationship between the strength and the width to height ratio. Again comparing it with the derived formula (see Fig 19c) it appears to be valid over a limited region. However, he does vere from the previously accepted power function formula and from the assumption that the strength curve must pass through the origin. On examining his experimental results more closely though, the start of an upward increase can be seen which fits a concave up curve far better than a straight line.

The limitations of these previous theories can be summed up as follows:-

(a). They are empirical and therefore cannot be extrapolated beyond the range over which they were derived (see Fig 19a).

(b). The power function theories are not dimensionally correct.

(c). Greenwald, Stoart and Bieniawski's formulae each applies only to a specific material under specific conditions.

(d). Salamon's and Munro's formula applies only to coals tested and due to the wide variety must of necessity contain a wide scatter.

(e). The power function formulae assume the strength curve to pass through the origin, which from experimental results does not appear to be the case.

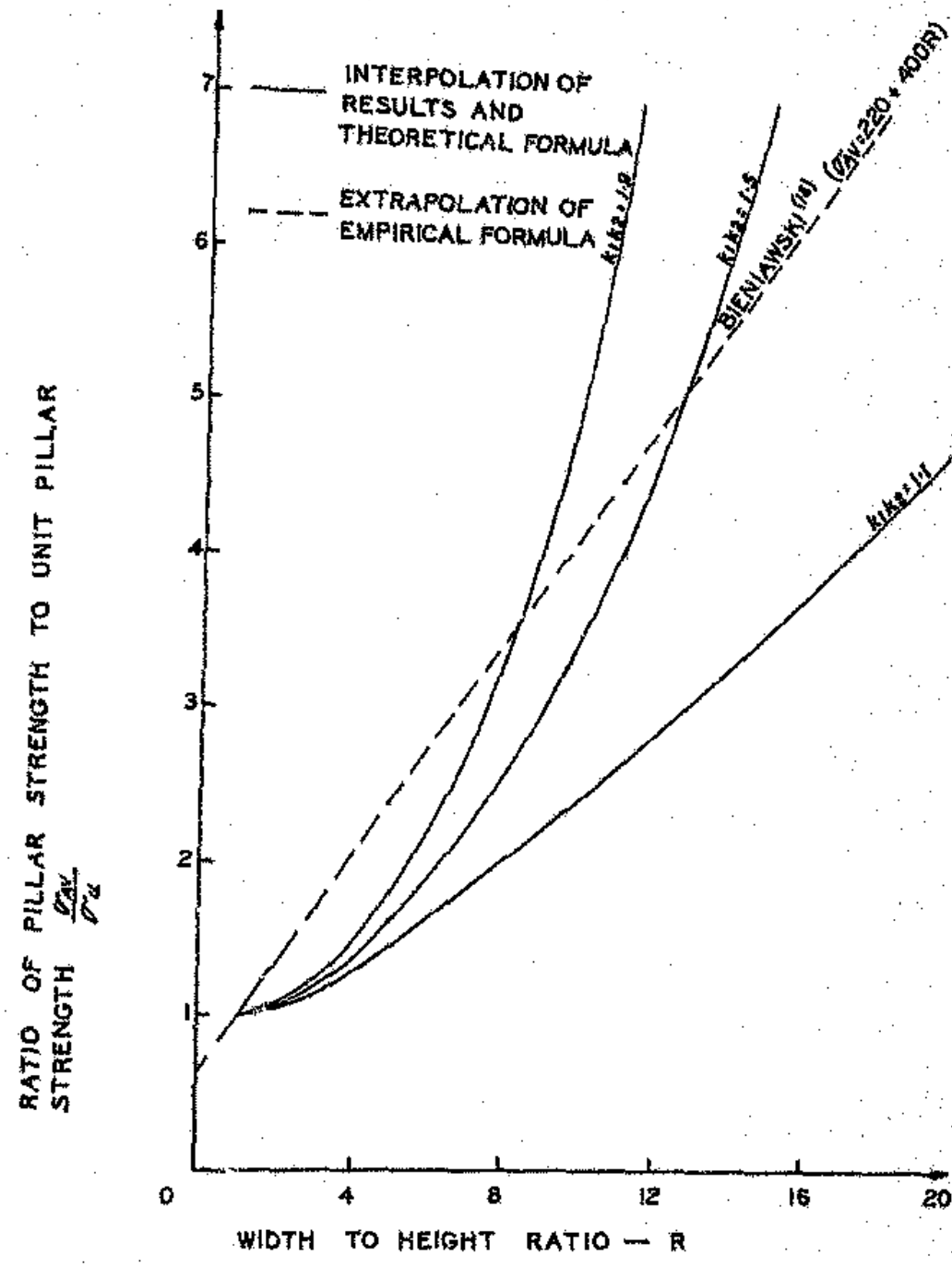


FIGURE 19c. COMPARISON OF THE "STRAIGHT LINE FORMULAE" TO THE POSTULATED THEORETICAL RELATIONSHIP.

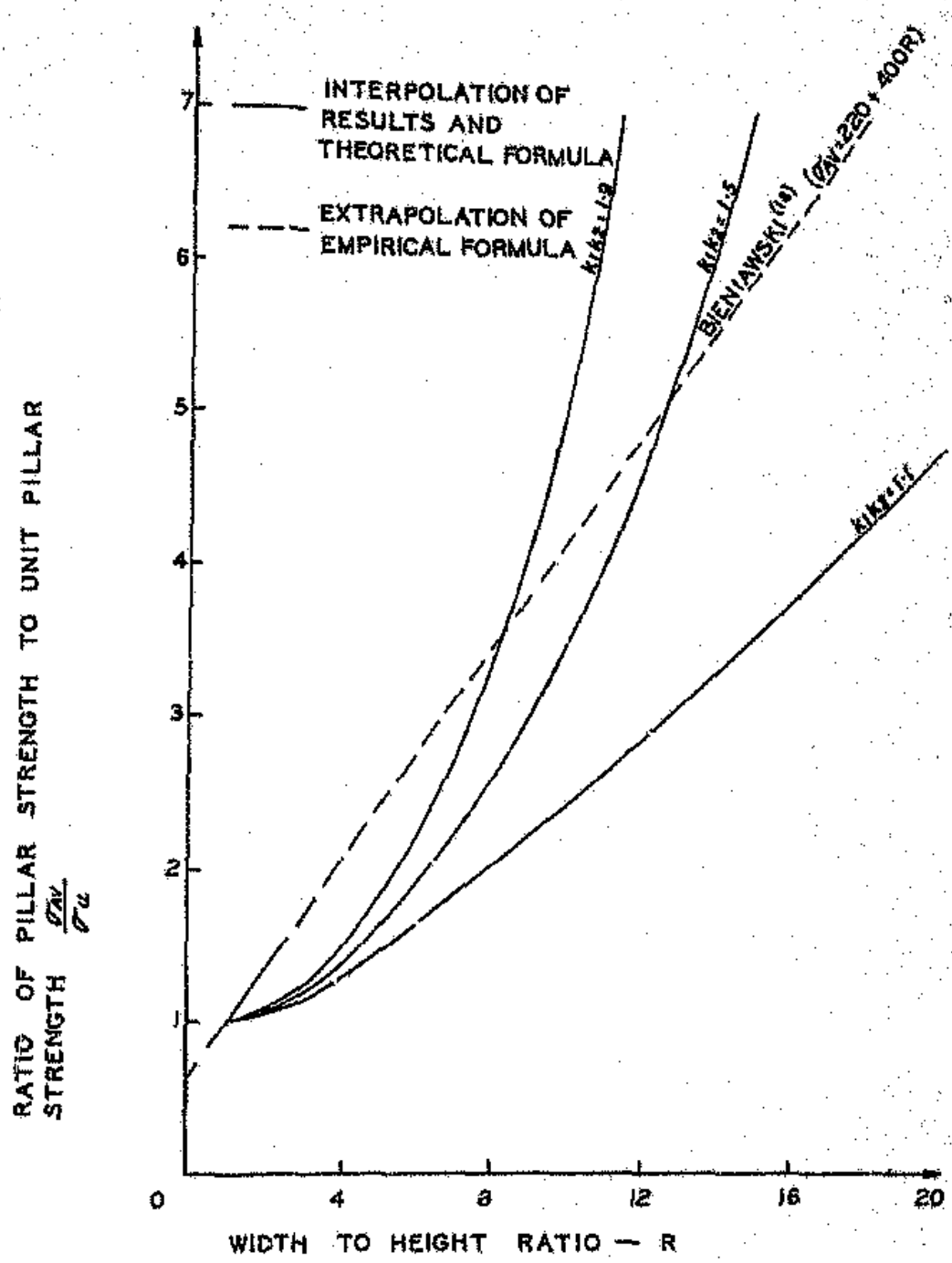


FIGURE 19c. COMPARISON OF THE "STRAIGHT LINE FORMULAE" TO THE POSTULATED THEORETICAL RELATIONSHIP.

9. CONCLUSIONS

Throughout this dissertation the emphasis has been on fundamental truths and first principles, working through generalisations to the specific.. In obtaining the specific, the broad view and encompassment of the generalisation is simplified where possible, making certain assumptions to provide a solution that is neither mathematically complex nor false through oversight in over-simplification.

The assumptions are made because, at this stage, their exact nature is not known nor can they be afforded to be ignored completely. The fact that they are acknowledged and their limitations are at present realised, serve to provide following researchers with well-defined problems which should prove to be of great assistance.

In enumerating the assumptions, it is hoped that should any discrepancy between theory and practice occur, a reassessment of the assumptions will provide the necessary change in results. The major assumptions are:-

(a). The material is homogeneous.

(b). The material is elastic.

(c). The values of k_1 and k_2 can be accurately obtained by preliminary tests on the material.

(d). The material will not change its properties due to its increased strength towards the centre of the pillar thus changing the values of k_1 and k_2.

(e). The strength of a unit pillar can be accurately obtained; either by a preliminary test on the unit pillar or by tests on a smaller specimen and the results confidently extrapolated.

(f). The average strength of the pillar is the true strength of the pillar, i.e. the stress at which the pillar finally fails is the same as the average strength of the pillar.

(g). The pillar remains intact until failure.

In assessing these assumptions with regard to deep level mines - the material is relatively homogeneous in the macroscopic state; previous researchers have found the rock to behave elastically; the product of k_1 and k_2 appears to be determinable and relatively constant; as a first approximation the strength of a unit pillar can be taken to be that of a specimen of testable size; and finally if the the pillar is large enough and rock which scales off at the sides is not removed, thus providing at least a token restraining effect which rapidly increases, then the pillar can be said to remain intact.

Therefore in using the proposed formulae first order results can be obtained for pillar strengths, resulting in a realistic approach in mine design. The pillar strength results need then only be modified slightly for the particular conditions by applying the relevent factors for which the information is gleaned from an accurate appraisal of the individual situation or, perhaps more important at this stage - experience.

The fact that the hypothesis bears up extremely well for laboratory results is no absolute criterion for its verity. What now remains is the ultimate test of the theory - that the proposed pillar strength formulae be used in the mines - with success.

ACKNOWLEDGMENTS

My thanks go to the Department of Mining Engineering at the University of the Witwatersrand for the use of their facilities, to the Chamber of Mines of South Africa for their financial assistance, to Professor R.P. Plewman and Mr. C. Grobbelaar whose constant supervision and advice were invaluable, especially to the latter who went to great lengths to correct the proofs, to various members of the staff who assisted on individual points and finally to Mrs. Hatfield who transformed the script into type.

References

1. COATES, D.F. Rock Mechanics Principles. Queen's Printer., Ottawa, 1965.

2. TIMOSHENKO, S and GOODIER, J.N. Theory of Elasticity. McGraw-Hill, New York 1951.

3. MUSKHELISHVELI, N.I. Some Basic Problems of the Mathematical Theory of Elasticity. P. Noordhoff Ltd, Groningen, Holland 3rd edition 1953.

4. OROWAN, E. 'Fracture and strength of solids'. Rept. Prog. Phys. Vol. 12, 1949.

5. GRIFFITH, A.A. 'The phenomena of rupture and flow in solids'. Phys. Trans. Royal Soc. A. Vol. 221, London 1921.

6. SACK, R.A. 'Extension of Griffith theory of rupture to three dimensions'. Proc. Phys. Soc. London, Vol. 58, 1946.

7. MC CLINTOCK, F.A. and WALSH, J.B. 'Friction on Griffith cracks in rock under pressure'. Inst. Cong. Appl. Mech. Berkeley, 1962.

8. HOFFMAN, O and SACKS Introduction to the Theory of Plasticity for Engineers. McGraw-Hill, New York 1953.

9. SALAMON, DR. M.D.G. 'Elastic analysis of displacements and and stresses induced by mining seam or reef deposits'. Symposium on Rock Mechanics and Strata Control in Mines. S.A.I.M.M. publication Johannesburg, 1965.

10. TERZAGHI, K and PECK, Soil Mechanics in Engineering Practice. Wiley, New York, 1948.

11. SALAMON, DR. M.D.G. and ORAVECZ, K.I. 'Mathematical analysis of stress and displacements around bord and pillar working'. Coal Mining Research Controlling Council. 51/65, Johannesburg, 1965.

12. WIGGILL, K.B. 'The effects of different support methods on strata behaviour around stoping excavations'. Symposium on Rock Mechanics and Strata Control S.A.I.M.M., Johannesburg, 1965.

13. LOGIE, C.V. 'Photoelastic model study into the ground stress in bord and pillar coal mining'. C.S.I.R. Report MEG. 439, Pretoria, 1966.

14. GREENWALD, H.P., HOWARTH, H.C. and HARTMANN, I. 'Experiments on the strength of small pillars of coal in the Pittsburgh Bed'. U.S. Bur. Min. Tech. . . . Pap. 606, 1939.

15. STEART, F.A. 'Strength and stability of pillars in coal mines'. J. Chem. Metall. Min. Soc. S.A., VOL. 54, 1954.

16. SALAMON, DR.M.D.G. and MUNRO, A.H. 'A study of the strength of coal pillars'. J. SA. Min. Metall., September 1967.

17. BIENIAWSKI, Z.T. 'The testing of large scale coal specimens in situ'. Rep. Coun. scient. ind. Res. S.Afr., no MEG 535, February 1967.

18. BIENIAWSKI, Z.T. 'An analysis of results from underground tests aimed at determining the in situ strength of coal pillars'. C.S.I.R. Report MEG.569, Pretoria, July 1967.

19. WIID, B.L. 'The influence of moisture on the strength behaviour of rock'. C.S.I.R. Report MEG.424, Pretoria, 1966.

20. HOEK, E. 'Rock fracture under static stress conditions'. C.S.I.R. Report MEG. 383, Pretoria, 1965.

21. GROBBELAAR, C. Unpublished paper.

APPENDIX 1

The Determination of k_1 under Elastic Conditions

The strength multiplication factor, k_1, can be determined for elastic conditions by use of the Mohr Rupture Diagram. The Mohr Rupture diagram in fig. 1a depicts the relationship between the maximum and minimum principal stresses, σ_1 and σ_3, at failure. This relationship can be plotted in graph form with σ_1 as the abscissa and σ_3 as the ordinate as shown in fig. 11b. At specific values the realtionship can be approximated to a straight line giving

$$\Delta\sigma_1 = k_1 \Delta\sigma_3$$

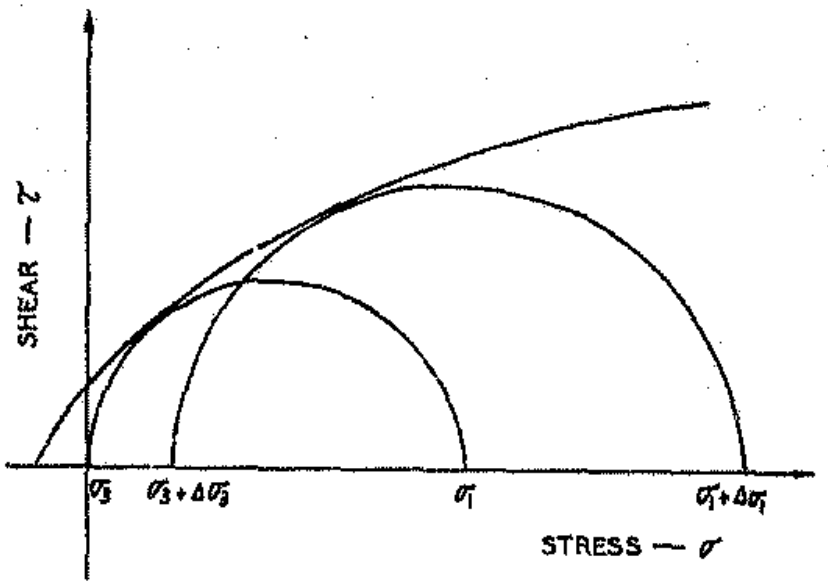


FIGURE Ia. MOHR RUPTURE DIAGRAM.

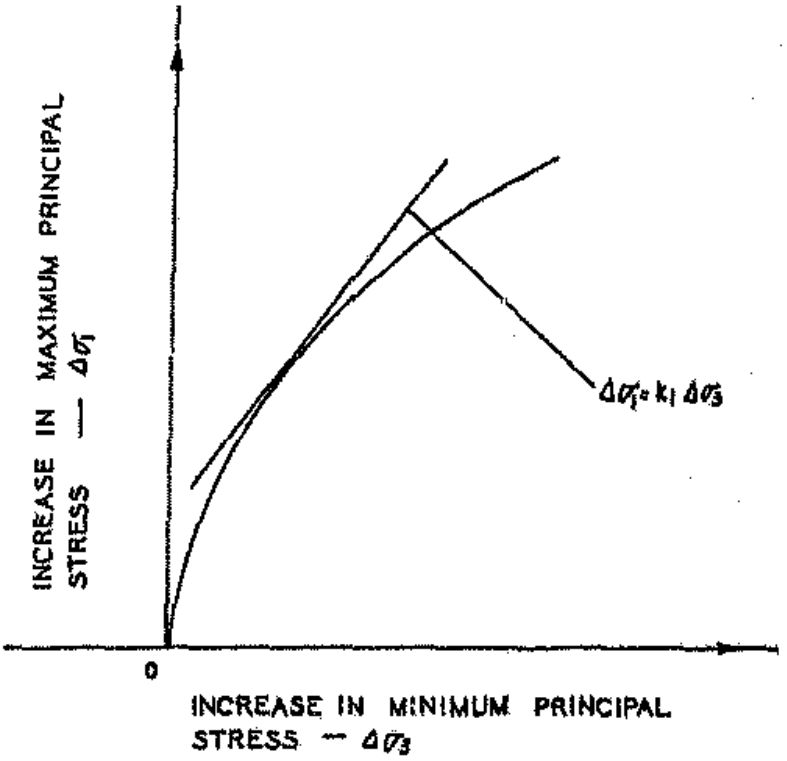


FIGURE Ib. DETERMINATION OF THE STRENGTH MULTIPLICATION FACTOR — k_1

APPENDIX II

The Determination of k_2 under Elastic Conditions

Under elastic conditions k_2 can be expressed in terms of the Poisson's Ratio ν. The relationship is derived from the generalised equation of elasticity.

$$y = \frac{\sigma_Y}{E} - \frac{\nu}{E}(\sigma_x + \sigma_z)$$

for the plane strain condition or the plane stress condition. k_2 lies between these 2 conditions.

(a). Plane Strain

As the body is restrained laterally $E_y = 0$; for complete lateral confinement the lateral stress is $\sigma_y = \sigma_z = \sigma_L$ and the vertical stress , $\sigma_x = \sigma_v$ giving the generalised equation of elasticity as

$$0 = \frac{\sigma_L}{E} - \frac{\nu}{E}(\sigma_v + \sigma_L)$$

$$\sigma_L - \nu\sigma_L = \nu\sigma_v$$

$$\sigma_L = \frac{\nu}{1-\nu}\sigma_v$$

But $$\sigma_L = k_2 \sigma_v$$

Therefore $k_2 = \frac{\nu}{1-\nu}$ for plane strain.

(b). Plane Stress

In the case of plane stress $\sigma_3 = 0$ and $\sigma_y = \sigma_L$ can vary between the limits of zero strain and zero stress. In the former case the body is restrained laterally, so $E_y = 0$; and $\sigma_x = \sigma_y$.

The generalised equation of elasticity becomes

$$0 = \frac{\sigma_L}{E} - \frac{\nu}{E}\ \sigma_v$$

$$\sigma_L = \nu\sigma_v$$

But $$\sigma_L = k_2\ \sigma_v$$

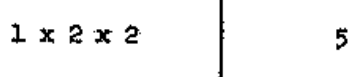
Therefore $k_2 = \nu$ for plane stress. If the y direction is also unrestrained $k_2 = 0$.

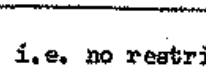
APPENDIX III

Validity of Approximation of Equal Strengths of all Unit Pillars in the Same Row in the Square Pillar Analysis

Dimension (Unit ratios)	No. of Readings	Load (Kilo lbs) Mean	Range
1 x 1 x 1	5	15.5	14.80 - 16.35
1 x 1 x 2	5	33.2	31.5 - 35.4
1 x 1 x 3	5	50.2	47.2 - 52.0
1 x 2 x 2	5	67.0	66.0 - 68.5
1 x 2 x 3	5	103.5	101.6 -105

i.e. no restriction  = 15.5

 = 2 x → restriction on 1 side →  = 16.6

 = 2 x →  + →  ← restriction on 2 opposite sides →  ←

= 17.0

 = 4 x →  restriction on 2 adjacent sides →  = 16.8

 = 4 x →  + 2 x →  ← restriction on 3 sides →  ← = 18.2

∴ Maximum error in approximating is $\frac{18.2 - 15.5}{15.5} = \frac{2.7}{15.5} = 17\%$

However, this is the difference between the corner block and the centre block, on one side of the pillar and the larger the $\frac{W}{H}$ ratio is the less the error will be.

Compared to the difference between no restriction and restriction on all four sides which is 150%, the error is negligible.

APPENDIX IV

Computor Program for Strip Pillar Calculation using the Continuous Rate of Increase Approach

```
      DIMENSION SIGMA(1000)
      READ 1,CBEG,CINT,CEND,RBEG,RINT,REND
    1 FORMAT(6F6.2)
      I=1
      C=CBEG
    7 V=ALOG(C)
      R=RBEG
    4 X=1.+(C**(R/2.)-C**0.5)*(C+1.)/(C*R*V*V)
      Y=(C**0.5+1./(C**0.5))*(R-1.)/(2.*R*V)
      SIGMA(I)=X-Y
      R=R+RINT
      IF(R-REND-0.01)2,2,3
    2 I=I+1
      GO TO 4
    3 PRINT 100,C,RBEG,RINT,REND
      PRINT 101,(SIGMA(J),J=1,I)
  100 FORMAT(//5H C=,F6.2,5X,2HR=,F6.2,1H,F6.2,1H,F6.2)
  101 FORMAT(/13E10.3)
      C=C+CINT
      IF(C-CEND-0.01)5,5,6
    5 I=1
      GO TO 7
    6 STOP
      END
```

Computor Program for Strip Pillar Plotter

```
      DIMENSION SIGMA(1000),DATA(4000)
      READ(5,1)CBEG,CINT,CEND,UNBEG,UNINT,UNEND
    1 FORMAT(6F6.2)
      CALL PLOTS(DATA(1),16000)
      CALL PLOT(1.0,-11.0,-3)
      CALL PLOT(0.0,0.5,-3)
      CALL AXIS(0.0,0.0,'AVERAGE STRENGTH/UNIT STRENGTH',30,10.0,
      90.0,0.0,2.0,10)
      CALL AXIS(0.0,0.0,'R',-1,10.0,0.0,1.0,1.0,10)
      I=1
      C=CBEG
    7 V=ALOG(C)
      CALL PLOT(0.0,0.0,3)
      UN=UNBEG
    4 X=1.+(C**(R/2.)-C**0.5)*(C+1.)/(C*R*V*V)
      Y=(C**0.5+1./(C**0.5))*(R-1.)/(2.*R*V)
      SIGMA(I)=X-Y
      SGPLT=SIGMA(I)*0.5
      VPLOT=VN-1.0
      IF(SGPLT-10.0)201,201,202
  201 CALL PLOT(VPLOT,SGPLT,2)
```

```
202     UN=UN+UNINT
        IF(UN-UNEND-0.01)2,2,3
  2     I=I+1
        GO TO 4
  3     C=C+CINT
        IF(C-CEND-0.01)5,5,6
  5     I=1
        GO TO 7
  6     CALL PLOT(12.0,0.0,999)
        STOP
        END
```

APPENDIX V

Comparison between the finite element approach and the continuous rate of increase approach in the determination of the strength of a wide strip piller.

The strength of pillars was calculated from two theoretical premises:- the summation of the effect of a number of individual elements, and the integration over the area of the pillar. The first is called the finite element (F.E.) approach and the second the continuous rate of increase (C.R.I.) approach.

In the table below, the ratios of the strengths of wide strip pillars to a unit pillar for various values of the width to height ratio (R) and of the strength factor k_1k_2 are given.

	k_1k_2 = 0.5		k_1k_2 = 1.0		k_1k_2 = 1.5	
R	F.E.	C.R.I.	F.E.	C.R.I.	F.E.	C.R.I.
1	1.00	1.00	1.00	1.00	1.00	1.00
3	1.17	1.20	1.33	1.33	1.50	1.39
5	1.35	1.56	1.80	1.80	2.35	2.09
7	1.43	1.76	2.29	2.29	3.52	3.06
9	1.58	1.90	2.78	2.78	5.10	4.37
11	1.65	2.00	3.27	3.27	7.28	6.15

The above data is shown graphically in figure 11.

The percentage difference between the two approaches is zero for k_1k_2 = 1.0 and varies according to the following table for k_1k_2 = 0.5 and 1.5. The percentages given are calculated as

$$100\ \frac{(\text{F.E.} - \text{C.R.I.})}{\text{C.R.I.}}$$

R	$k_1k_2 = 0.5$	$k_1k_2 = 1.5$
1	0.0%	0.0%
3	- 8.6%	7.2%
5	-13.5%	12.4%
7	-15.9%	15.0%
9	-16.8%	16.7%
11	-17.5%	18.4%

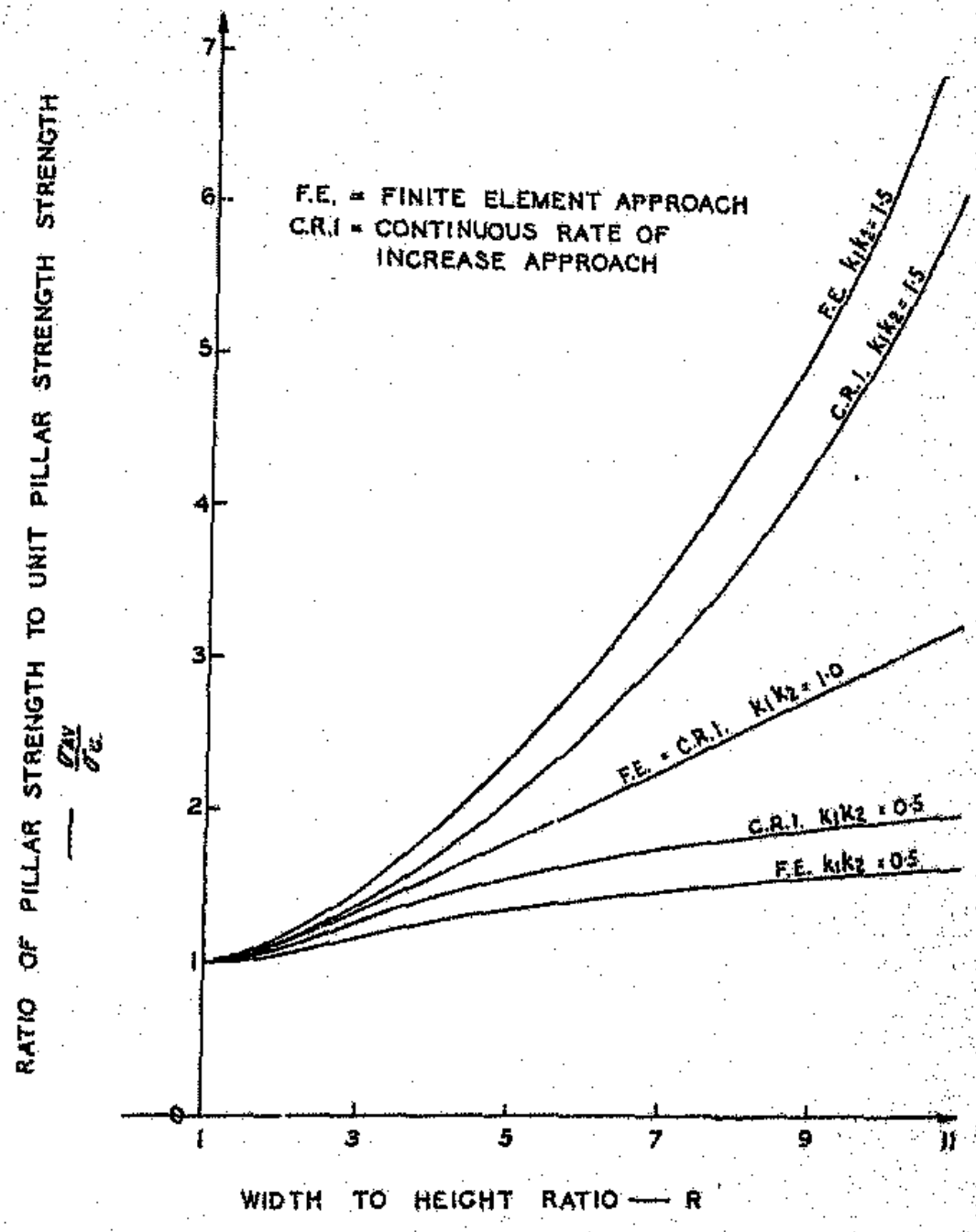


FIGURE II. COMPARISON OF THE FINITE ELEMENT APPROACH TO THE CONTINUOUS RATE OF INCREASE APPROACH.

APPENDIX VI

The square pillar formula as a continuous function

In order to obtain values for R other than odd integers, the discreet finite element function

$$\sum_{r=0}^{\frac{R-1}{2}} \left(1-\frac{2r}{R}\right)^2 c^r \qquad 1$$

can be approximated by a continuous function. This function can be programmed to give a value for any value of R, c being specified.

Function 1 can be written as

$$\sum_{r=0}^{\frac{R-1}{2}} \frac{1}{R^2} (R-2r)^2 c^r$$

$$= \frac{1}{R^2} \sum_{r=0}^{\frac{R-1}{2}} (R-2r)^2 c^r$$

Replacing the summation by an integral and taking limits from $-\frac{1}{2}$ to $\frac{R}{2}$, we get

$$\frac{1}{R^2} \int_{-\frac{1}{2}}^{\frac{R}{2}} (R-2x)^2 c^x dx$$

However, on evaluation, the approximation differs most widely at R=1, and as at R=1 the function must equal 1, we rewrite it, making the necessary change in the limit, as

$$1 + \frac{1}{R^2} \int_{\frac{1}{2}}^{\frac{R}{2}} (R-2x)^2 c^x dx$$

N.B. When R = 1, $\int = 0$ and therefore the function equals unity.

i.e. $\frac{\sigma}{\sigma_0} = 1$

Expanding the equation

$$\frac{\sigma}{\sigma_o} = 1 + \frac{1}{R^2}\int_{\frac{1}{2}}^{\frac{R}{2}} (R-2x)^2 c^x dx$$

we get

$$= 1 + \frac{1}{R^2}\int_{\frac{1}{2}}^{\frac{R}{2}} (R^2 - 4Rx + 4x^2)\, c^x dx$$

$$= 1 + \frac{1}{R^2}\left[\int_{\frac{1}{2}}^{\frac{R}{2}} R^2 c^x dx - \int_{\frac{1}{2}}^{\frac{R}{2}} 4Rxc^x dx + \int_{\frac{1}{2}}^{\frac{R}{2}} 4x^2 c^x dx\right]$$

integrating

$$= 1 + \frac{1}{R^2}\left[\left|\frac{R^2 c^x}{\log c}\right|_{\frac{1}{2}}^{\frac{R}{2}} - \left|\frac{4Rxc^x}{\log c} - \frac{4Rc^x}{\log^2 c}\right|_{\frac{1}{2}}^{\frac{R}{2}} + \left|\frac{4x^2 c^x}{\log c} - \frac{x}{\log^2 c} + \frac{8c^x}{\log^3 c}\right|_{\frac{1}{2}}^{\frac{R}{2}}\right]$$

evaluating

$$= 1 + \frac{c}{R^2}^{\frac{R}{2}}\left[\frac{R^2 - 2R^2 + R^2}{\log c} + \frac{4R-4R}{\log^2 c} + \frac{8}{\log^3 c}\right]$$

$$+ \frac{c}{R^2}^{\frac{1}{2}}\left[\frac{R^2 - 2R + 1}{\log c} + \frac{4R-4}{\log^2 c} + \frac{8}{\log^3 c}\right]$$

$$\therefore \frac{\sigma}{\sigma_o} = 1 + \frac{c}{R^2}^{\frac{R}{2}}\left[\frac{8}{\log^3 c}\right] - \frac{c}{R^2}^{\frac{1}{2}}\left[\frac{(R-1)^2}{\log c} + \frac{4(R-1)}{\log^2 c} + \frac{8}{\log^3 c}\right] \quad (1)$$

This equation holds for $c > o$ and $c \neq 1$. It approximates function 1 for all values of $R \geq 1$.

N.B. By definition $c \leq o$ is meaningless, and in nature $c > 2.5$ is rare.

For the special case of $c = 1$ function 1 becomes

$$\sum_{r=0}^{\frac{R-1}{2}} \left(1-\frac{2r}{R}\right)^2 \qquad 2.$$

Function 2 can be approximated by the integral

$$1 + \frac{1}{R^2}\int_{\frac{1}{2}}^{\frac{R}{2}} (R-2x)^2 dx$$

giving the equation

$$\frac{\sigma}{\sigma_o} = 1 + \frac{1}{R^2}\int_{\frac{1}{2}}^{\frac{R}{2}} (R^2 - 4Rx + 4x^2)\, dx$$

$$= 1 + \frac{1}{R^2}\left[R^2 x - 2Rx^2 + \frac{4x^3}{3}\right]_{\frac{1}{2}}^{\frac{R}{2}}$$

$$= 1 + \frac{1}{R^2}\left[\frac{R^3}{2} - \frac{R^3}{2} + \frac{R^3}{6}\right] - \frac{1}{R^2}\left[\frac{R^2}{2} - \frac{R}{2} + \frac{1}{6}\right]$$

$$\therefore \frac{\sigma}{\sigma_o} = 1 + \frac{1}{R^2}\left[\frac{R^3}{6} - \frac{R^2}{2} + \frac{R}{2} - \frac{1}{6}\right] \qquad (B)$$

The general equation A can be programmed for an IBM 360 computer to give a set of values for $\frac{\sigma}{\sigma_o}$ for various c values and R values. It can also be programmed to plot various c curves on a width to height ratio - $\frac{\sigma}{\sigma_o}$ graph.

APPENDIX VII

Specimen Saturation Times

(for various thicknesses)

Time (mins)	Mass of Specimen (grams)			
	2"	1"	½"	¼"
0	604.4	177.0	138.6	53.4
30	622.5	189.4	144.5	56.1
60	625.5	189.5	144.5	56.0
180	626.3	189.9	144.7	56.0

Time (mins)	Mass of Specimen (grams)		
	1"	½"	¼"
0	168.8	142.7	47.1
5	178.3	148.4	51.3
10	181.0	148.6	51.3
15	181.1	148.5	51.4

Time (mins)	Mass (grams) ¼"
0	88.8
1	92.5
2	92.6

Drying Times (for ½" thickness)

Time (mins)	Mass (grams)
0	81.3
1	81.1
2	81.0
3	81.0
4	81.0

Time (mins)	Mass (grams)
6	80.9
7	80.9
8	80.9
9	80.9
10	80.9
1110	77.8

APPENDIX VIII

THE EFFECT OF INTERFACES ON THE FAILURE LOAD

Model	Number of Specimens tested	Failure Load	
		Mean	Range
Solid	3	52.7	47.1 - 59.0
No filling	2	16.9	15.2 - 18.6
P/P filling	3	22.8	19.8 - 24.4
Araldite filling	2	20.6	19.7 - 21.5

Platten	Number of Specimens tested	Load	
		Mean	Range
Sandstone	5	43.3	38.4 - 49.3
Metal	5	42.4	37.2 - 47.7

APPENDIX IX

Strip Pillar Problem

What size of pillar is required to support 10,000 feet of rock?

Rock density = 167 lb/cu.ft.

$\nu = 0.15$

$k_1 = 8.5$

Stoping width = 4 ft.

Strength of a 4 ft. cube = 40,000 p.s.i.

Maximum span = 200 ft.

Solution

a). Strength curve using finite element approach

$k_1 = 8.5$

$k_2 = \frac{\nu}{1-\nu} = \frac{0.15}{0.85}$

$c = k_1 k_2 = 1.5$

For $R = 1 \quad \sigma_{AV} = \sigma_u = 40{,}000$ p.s.i.

$R = 3 \quad \sigma_{AV} = \sigma_u(1+\frac{c}{3}) = 60{,}000$ p.s.i.

$R = 5 \quad \sigma_{AV} = \sigma_u(1+\frac{3c}{5}+\frac{c}{5}^2) = 94{,}000$ p.s.i.

$R = 7 \quad \sigma_{AV} = \sigma_u(1+\frac{5c}{7}+\frac{3c}{7}^2+\frac{c}{7}^3) = 140{,}000$ p.s.i.

b). Strength curve using continuous rate of increase approach

$k_1 = 8.5$

$k_2 = \frac{\nu}{1-\nu} = \frac{0.15}{0.85}$

$c = k_1 k_2 = 1.5$

/ From

From the equation

$$\frac{\sigma_{AV}}{\sigma_u} = 1 + \frac{(c^{\frac{R}{2}} - c^{\frac{1}{2}})(c+1)}{c\,R \log c} - \frac{(c^{\frac{1}{2}} + c^{-\frac{1}{2}})(R-1)}{2R \log c}$$

for $c = 1.5$ or from the graph for $k_1 k_2 = 1.5$ in fig

For

R = 1	σ_{AV}	= σ_u =	40,000 p.s.i.
R = 2	σ_{AV}	= 1.14 σ_u =	46,000 p.s.i.
R = 3	σ_{AV}	= 1.39 σ_u =	56,000 p.s.i.
R = 4	σ_{AV}	= 1.71 σ_u =	68,000 p.s.i.
R = 5	σ_{AV}	= 2.09 σ_u =	84,000 p.s.i.
R = 6	σ_{AV}	= 2.54 σ_u =	102,000 p.s.i.
R = 7	σ_{AV}	= 3.06 σ_u =	122,000 p.s.i.

c). Load curve for strip pillar

$$\text{Virgin stress} - \sigma_o = \frac{167 \text{ lbs/ft}^3 \times 10{,}000 \text{ ft}}{144 \text{ ins}^2/\text{ft}^2}$$

$$= 11{,}600 \text{ p.s.i.}$$

From diagram in figure 111

$$\text{Percentage extraction} = x = \frac{200}{200 + v} \times 100$$

$$\text{load} = \frac{100}{100 - x} \times \sigma_o$$

For R = 5 i.e. v = 20

$$x = \frac{200}{200 + 20} \times 100 = 90.9\%$$

$$\text{Load} = \frac{100}{100-90.9} \times 11{,}600 = 128{,}000 \text{ p.s.i.}$$

R = 6 load = 108,000 p.s.i.

R = 7 load = 95,000 p.s.i.

From the graphs of the strength curve and the load curve shown in figures 111 and 1V it can be seen that the point of intersection is the optimum point for design i.e. the smallest pillar (thereby giving the greatest extraction ratio) that can support the load of the overlying rock. By choosing a pillar size larger than the optimum, a factor of safety is introduced.

For Finite Element Approach (see fig. 111)

Optimum size is R = 5.75 i.e width = 23 ft. Designing for R = 7 i.e. width = 28 ft, % extraction = 88%.

Safety factor = $\frac{140,000}{95,000}$ p.s.i. = 1.47

For Continuous Rate of Increase Approach (see fig. 1V)

Optimum size is R = 6.2 i.e. width = 25 ft. Designing for R = 7, i.e. width = 28 ft, % extraction = 88%

Safety factor = $\frac{122,000}{95,000}$ p.s.i. = 1.28

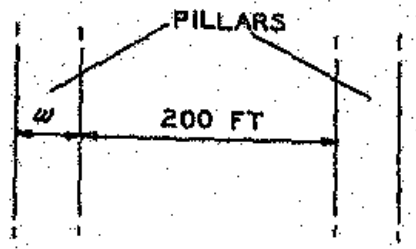


DIAGRAM OF STRIP PILLAR PLAN.

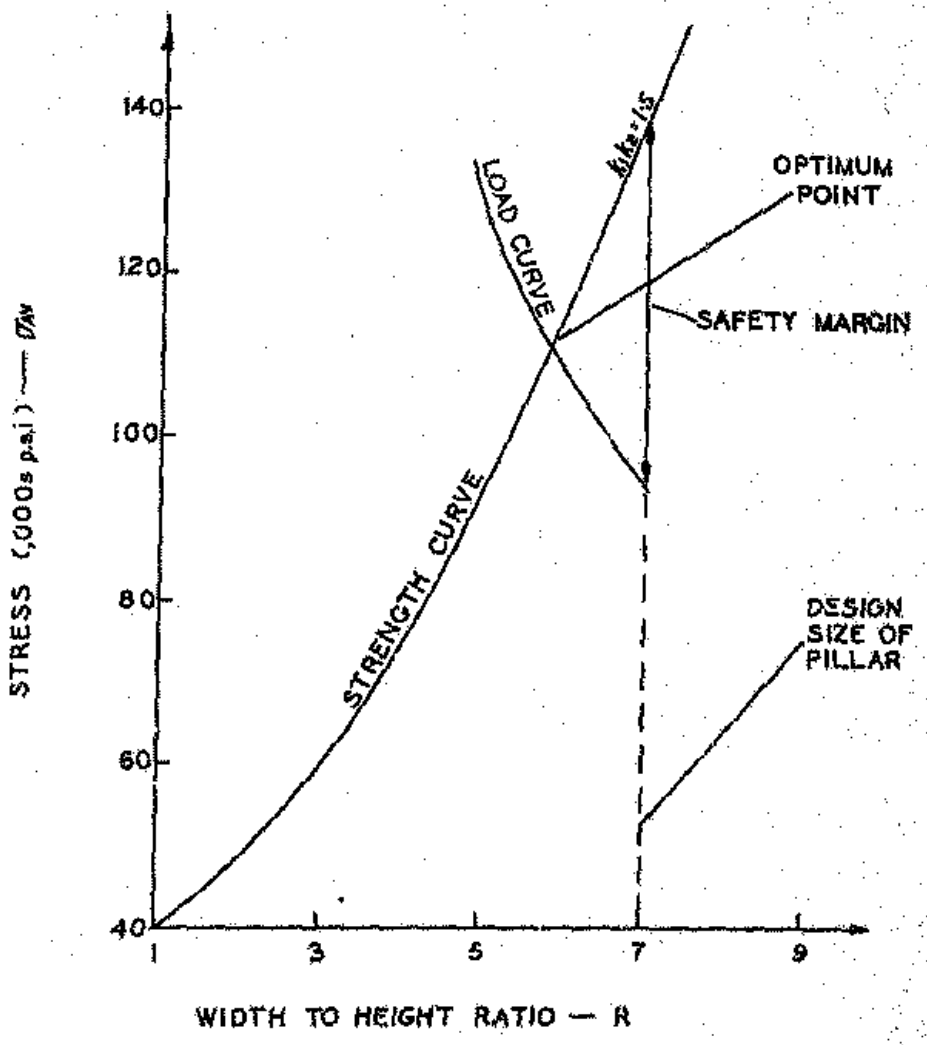


FIGURE III THE STRENGTH AND LOAD CURVES FOR A WIDE STRIP PILLAR USING THE FINITE ELEMENT APPROACH.

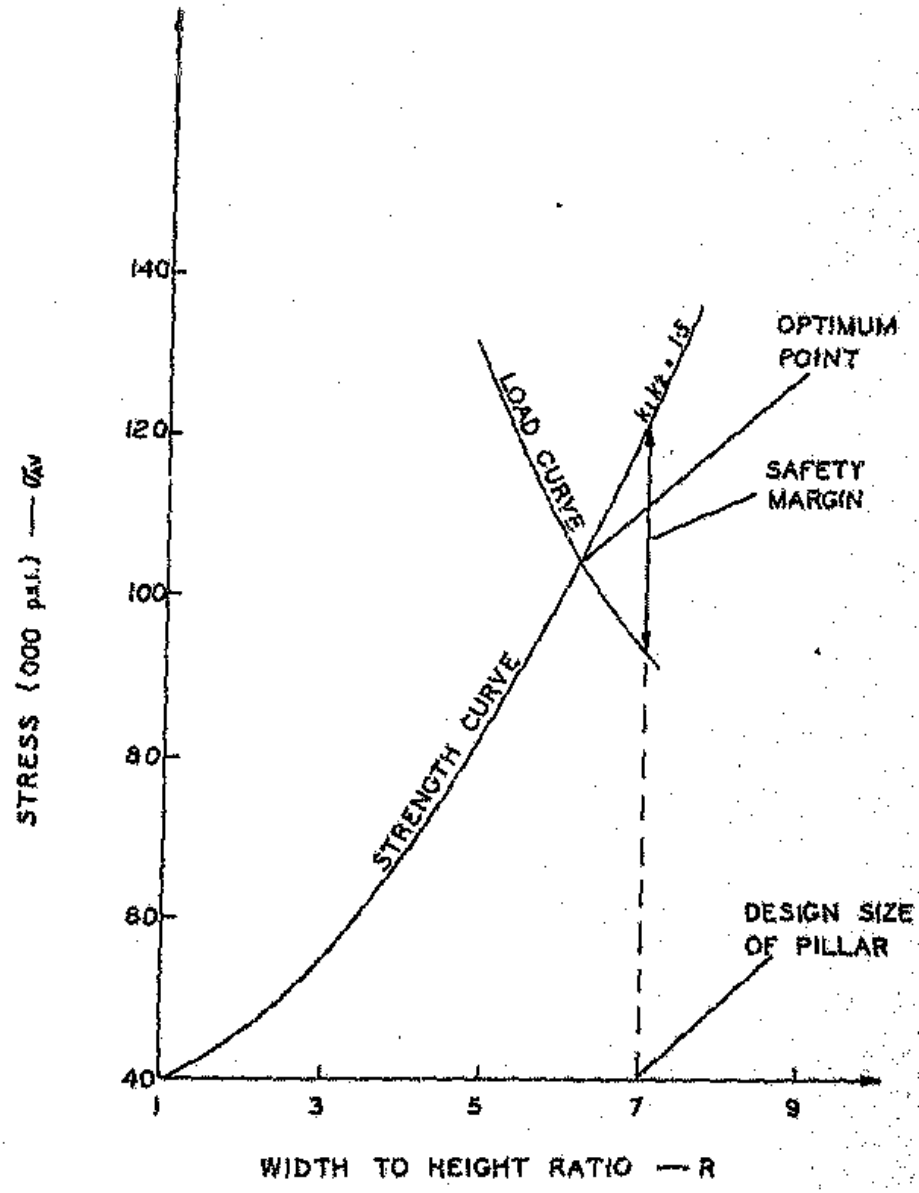


FIGURE IV THE STRENGTH AND LOAD CURVES FOR A WIDE STRIP PILLAR USING THE CONTINUOUS RATE OF INCREASE APPROACH.

Square Pillar Problem

Problem

What size of pillar is required to support 10,000 feet of rock?

Rock density = 167 lb/cu.ft.

$\nu = 0.15$

$k_1 = 8.5.$

Stoping width = 4 ft.

Strength of a 4 ft cube. = 40,000 p.s.i.

Maximum span = 200 ft.

Solution

(a). Strength Curve

$$k_1 = 8.5.$$

$$k_2 = \frac{\nu}{1-\nu} = \frac{0.15}{0.85}$$

$$c = k_1 k_2 = 1.5$$

For

$R = 1 \quad \sigma_{AV} = \sigma_u = 40{,}000$ p.s.i.

$R = 3 \quad \sigma_{AV} = \sigma_u \left(1+\frac{c}{9}\right) = 47{,}000$ p.s.i.

$R = 5 \quad \sigma_{AV} = \sigma_u \left(1 + \frac{9c}{25} + \frac{c}{25}^2\right) = 55{,}000$ p.s.i.

$R = 7 \quad \sigma_{AV} = \sigma_u \left(1 + \frac{25c}{49} + \frac{9c^2}{49} + \frac{c^3}{49}\right) = 90{,}000$ p.s.i.

$R = 9 \quad \sigma_{AV} = \sigma_u \left(1 + \frac{49c}{81} + \frac{25c}{81}^2 + \frac{9c}{81}^3 + \frac{c}{81}^4\right) = 122{,}000$ p.s.i.

$R = 11 \quad \sigma_{AV} = \sigma_u \left(1 + \frac{81c}{121} + \frac{49c}{121}^2 + \frac{25c}{121}^3 + \frac{9c}{121}^4 + \frac{c}{121}^5\right) = 162{,}000$ p.s.i.

$R = 13 \quad \sigma_{AV} = \sigma_u \left(1 + \frac{121c}{169} + \frac{81c}{169}^2 + \frac{49c}{169}^3 + \frac{25c}{169}^4 + \frac{9c}{169}^5 + \frac{c}{169}^6\right) = 214{,}000$ p.s.i.

(b). Load Curve for Square Pillar

$$\text{Virgin stress } \sigma_o = \frac{167 \text{ lbs/ft}^3 \times 10{,}000 \text{ ft}}{144 \text{ ins}^2/\text{ft}^2}$$

$$= 11{,}600 \text{ p.s.i.}$$

From diagram in fig IV

$$\text{Percentage extraction} - x = \frac{(140 + w)^2 - w^2}{(140 + w)^2} \times 100$$

$$\text{Load} = \frac{100}{100-x} \times \sigma_o$$

For R = 10 i.e. w = 40 ft.

$$x = \frac{(140 + 40)^2 - 40^2}{(140 + 40)^2} \times 100 = 95.1\%$$

$$\text{Load} = \frac{100}{100-95.1} \times 11{,}600 = 237{,}000 \text{ p.s.i.}$$

R = 11 load = 203,000 p.s.i.

R = 12 load = 178,000 p.s.i.

R = 13 load = 155,000 p.s.i.

From the graph of strength curve and load curve shown in fig. V:-

Optimum size is R = 11.8, i.e. width 47 ft. Designing for R = 13, i.e. width = 52 ft, % extraction 92.5%

$$\text{Safety} = \frac{214{,}000}{155{,}000} = 1.38$$

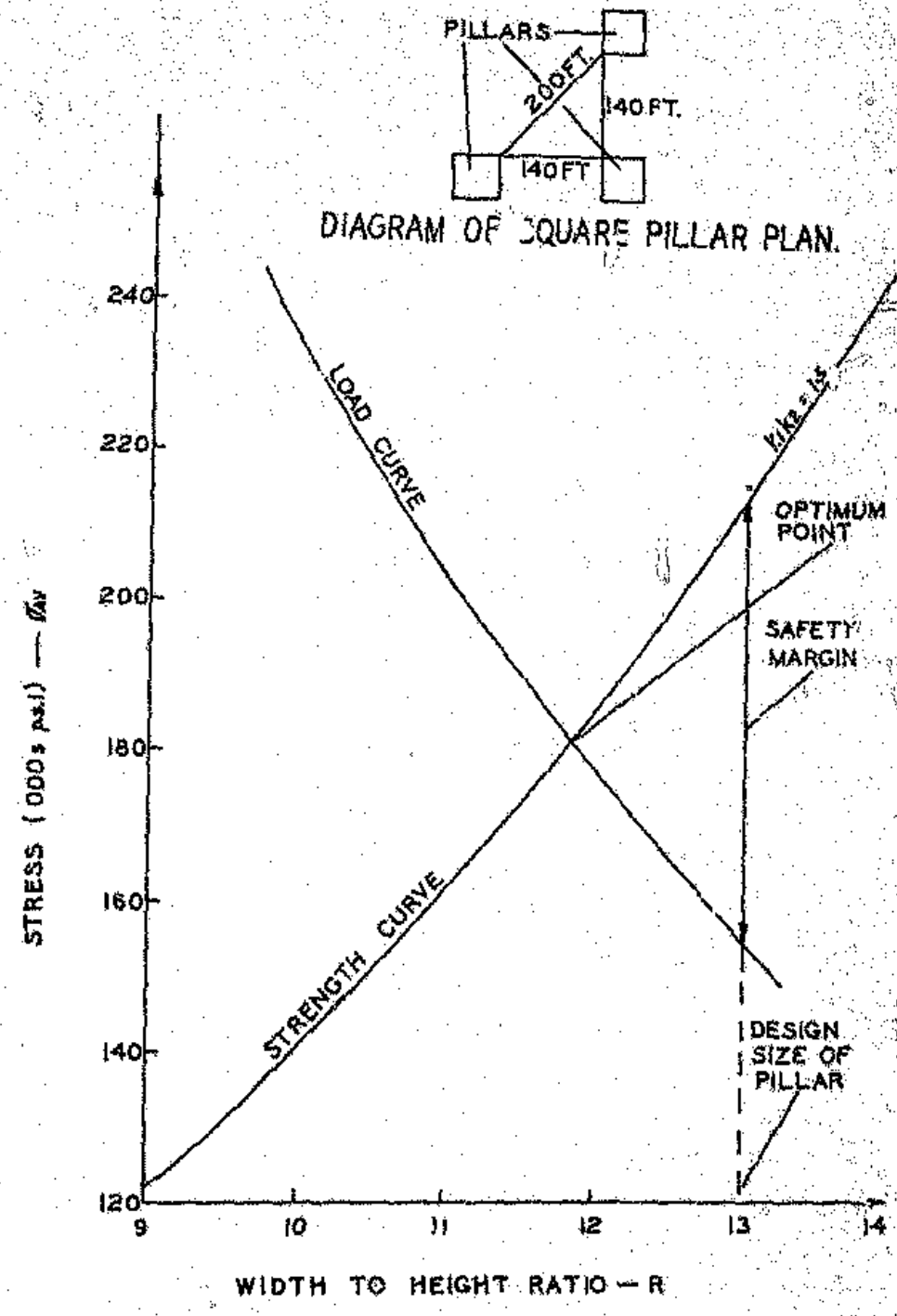


FIGURE V THE STRENGTH AND LOAD CURVES FOR A WIDE SQUARE PILLAR.

APPENDIX XI

Circular Pillar Problem

Problem

What size of pillar is required to support 10,000 feet of rock?

Rock density	=	167 lbs/cu. ft.
ν	=	0.15
k_1	=	8.5
Stoping width	=	4 ft.
Strength of a 4ft.cube	=	40,000 p.s.i.
Maximum span	=	200 ft.

Solution

(a). Strength Curve

$$k_1 = 8.5$$

$$k_2 = \frac{\nu}{1-\nu} = \frac{0.15}{0.85}$$

$$c = k_1 k_2 = 1.5$$

From the equation

$$\frac{\sigma_{AV}}{\sigma_u} = 1 + \frac{c^{r} + c^{r-1}}{r^2 \log^3 c} - \frac{c^{\frac{1}{2}} + c^{-\frac{1}{2}}}{r^2} - \frac{(r-\frac{1}{2})^2}{2\log c} + \frac{(r-\frac{1}{2})}{\log^2 c} + \frac{1}{\log^3 c}$$

R = 1	i.e. $r = \frac{1}{2}$	σ_{AV} =	σ_u	= 40,000 p.s.i.
R = 10		σ_{AV} = 3.10	σ_u	= 124,000 p.s.i.
R = 12		σ_{AV} = 4.05	σ_u	= 162,000 p.s.i.
R = 14		σ_{AV} = 5.28	σ_u	= 211,000 p.s.i.

(b). Load Curve for Circular Pillar

$$\text{Virgin stress} - \sigma_o = \frac{167 \text{lbs/ft}^3 \times 10{,}000 \text{ ft}}{144 \text{ ins}^2/\text{ft}^2}$$

$$= 11{,}600 \text{ p.s.i.}$$

From diagram in fig. V1

$$\text{Percentage extraction} - x = \frac{(140 + 1.4r)^2 - r^2}{(140 + 1.4r)^2} \times 100$$

$$\text{Load} = \frac{100}{100 - x} \times \sigma_o$$

For R = 12 i.e. r = 24

$$x = \frac{(140 + 34)^2 \times 24^2 \pi}{(140 + 34)^2} = 94.1\%$$

$$\text{Load} = \frac{100}{100 - 94.1} \times 11{,}600 \text{ p.s.i.} = 197{,}000$$

R = 13 Load = 170,000

R = 14 Load = 155,000

From the graph of strength curve and load curve shown in fig. V1:-

Optimum size is R = 12.7 i.e. radius = 25 ft. Designing for R = 14, i.e. radius = 28 ft, % extraction = 92.5%

$$\text{Safety factor} = \frac{211{,}000 \text{ p.s.i}}{151{,}000 \text{ p.s.i.}} = 1.40$$

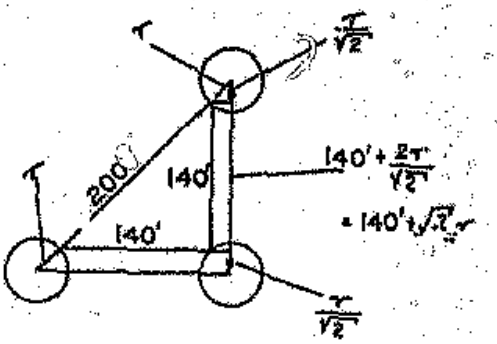


DIAGRAM OF CIRCULAR PILLAR PLAN.

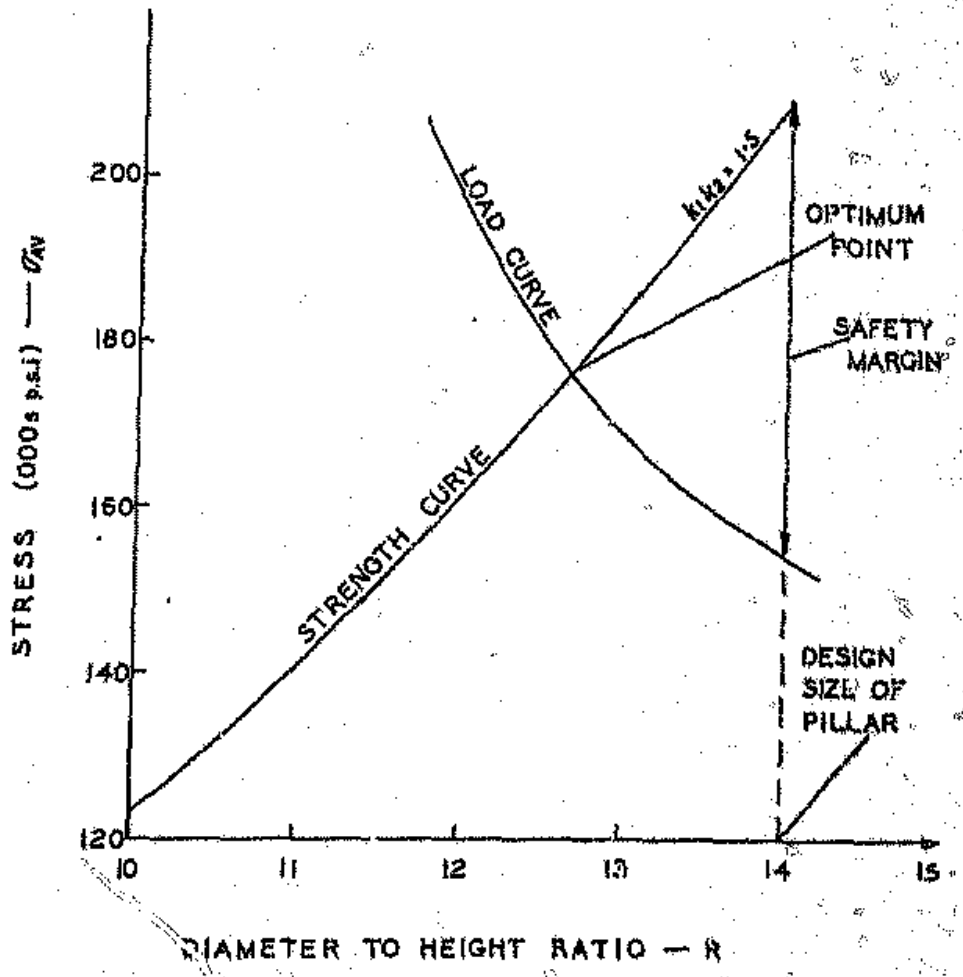


FIGURE VI. THE STRENGTH AND LOAD CURVES FOR A WIDE CIRCULAR PILLAR.

Author Cruise John Anthony
Name of thesis The determination of the strength characteristics of wide pillars. 1969

PUBLISHER:
University of the Witwatersrand, Johannesburg
©2013

LEGAL NOTICES:

Copyright Notice: All materials on the University of the Witwatersrand, Johannesburg Library website are protected by South African copyright law and may not be distributed, transmitted, displayed, or otherwise published in any format, without the prior written permission of the copyright owner.

Disclaimer and Terms of Use: Provided that you maintain all copyright and other notices contained therein, you may download material (one machine readable copy and one print copy per page) for your personal and/or educational non-commercial use only.

The University of the Witwatersrand, Johannesburg, is not responsible for any errors or omissions and excludes any and all liability for any errors in or omissions from the information on the Library website.